AD NUMBER

AD456378

LIMITATION CHANGES

TO:

Approved for public release; distribution is unlimited.

FROM:

**Distribution authorized to U.S. Gov't. agencies and their contractors;
Administrative/Operational Use; JAN 1965. Other requests shall be referred to Office of Naval Research, Washington, DC 20360.**

AUTHORITY

ONR Itr, 4 May 197

AD_ 456378

456378

LASER MATERIALS

TECHNICAL SUMMARY REPORT
Covering Period from 1 April through 31 December 1964

Contract Nonr-4130(00) A1
ARPA Order Number 306
Project Code Number 3730
Task Number NR017-707

A 12-Month Contract
From 1 April 1964 through 31 March 1965

30 January 1965

This research is part of Project DEFENDER under the joint sponsorship of the Advanced Research Projects Agency, the Office of Naval Research, and the Department of Defense

KORAD CORPORATION
A Subsidiary of Union Carbide Corporation
2520 Colorado Avenue
Santa Monica, California

L A S E R M A T E R I A L S

TECHNICAL SUMMARY REPORT
Covering Period from 1 April through 31 December 1964

Contract Nonr-4130(00) A1
ARPA Order Number 306
Project Code Number 3730
Task Number NR017-707

A 12-Month Contract
From 1 April 1964 through 31 March 1965
Total Contract Cost: $ 339,220

Principal Investigators
R. H. Hoskins
R. C. Pastor

KORAD CORPORATION
A Subsidiary of Union Carbide Corporation
2520 Colorado Avenue
Santa Monica, California
213 - 393-6737

TABLE OF CONTENTS

LIST OF FIGURES

L A S E R M A T E R I A L S

Section 1
INTRODUCTION

The objective of this program is the development of new laser materials. The approach being taken has been divided into three separate phases, as follows:

PHASE A - the search, synthesis, and crystal growth of suitable candidates for laser host materials,

PHASE B - the synthesis and crystal growth of such systems, consisting of the host and a chosen activator, and

PHASE C - the materials evaluation of these systems through measurement of relevant spectroscopic properties.

The host materials under investigation are Y_2O_3, $LaAlO_3$, and $YAlO_3$. The levels of success achieved with these three materials during the report period are briefly summarized in the following paragraphs and outlined in detail in the main text.

Significant strides have been made in the powder, the burner (design), and the muffle (design and structural stability) technologies for Y_2O_3. These advancements have progressed the state of the art in host crystal growth by the conventional Verneuil method from $\sim$ 1/16 inch diameter to $\sim$ 1/2 inch diameter. They have, in addition, been attained in an interval of less than one year from the time laser action was first achieved with $Y_2O_3:Nd^{+3}$.

Although yttria has a melting point much higher than that of corundum (2450° vs 2050° C), it is important to note that the pace of progress with yttria compares favorably with the improvements obtained in ruby at a similar stage of development.

The room temperature laser threshold of $Y_2O_3:Nd^{+3}$ at its present point of development is approximately twice that of CW-quality $CaWO_4$ of a similar size and concentration.

With regard to ABO_3 ($LaAlO_3$ and $YAlO_3$), the most significant achievement has been in the chemistry of materials. Various schemes have been worked out and procedures developed for the preparation of a truly stoichiometric feed. The question of congruency has been resolved ($LaAlO_3$ in favor of $YAlO_3$). And this has provided a capability for conducting a quick exploration of congruence between the two types of stoichiometry (ABO_3 and $A_3B_5O_{12}$, where A = rare earth, B = Al or Ga, etc.).

A recent improvement in flowability will now permit the study of further refinements in the crystal quality of $LaAlO_3$ and the problem of stability.

Corrosion studies fundamental to the growth of $LaAlO_3$ by the Czochralski method have yielded positive results, and crystal growth runs using this technique should soon be in operation.

Section 2
UNARY HOST OXIDE - Y_2O_3

A. Synthesis and Crystal Growth

The Final Report covering work performed during the preceding contract period[1] indicated that the problems still outstanding in the crystal growth of yttria were:

> the achievement of a higher level of absolute purity in the starting material, and
>
> the attainment and maintenance of a more favorable heat balance under steady state conditions of growth throughout a time interval commensurate with the size of the monocrystal.

(1) Chemistry of Materials

The starting purity of yttria powder is a very sensitive factor in the scale-up and quality improvement of the crystal. With regard to the problem of purity, the effects of various impurities in the product were first realized as gradual improvements in crystal quality were achieved. Some of these impurities were innocuous, others were extremely undesirable. The use of ionizing radiations (e.g., flashlamp excitation) indicated marked changes in absorption (color centers) with the presence of certain rare earth impurities which were distinctly polyvalent (e.g., terbium, ytterbium, etc.). Similar degradation could, essentially, be manifested by (or controlled to a certain extent for) some of these

---

1 Final Report, Contract Nonr-4130(00), "Laser Materials", dated 30 April 1964, covering 12-month contract period from 1 April 1963 through 31 March 1964.

impurities by means of a redox treatment. The spectrum of impurities within the purity rating of various materials therefore became a very significant factor.

Inasmuch as a search for an absolutely clean source of yttria appeared highly unrealistic, we undertook the more selective approach of studying the impurity spectrum. A survey study of yttria sources was conducted toward the objective of matching the economics and technology of outside-source materials with that obtainable in our own laboratory (viz., further purification in-house) in order to provide the optimum material for crystal growth. The results of this survey are given in Appendix I. The study determined that emission spectroscopy alone cannot provide a basis for selection from the various materials to the degree of refinement exacted by crystal growth. Selection was achieved through an interplay of various in-house capabilities. Considering the uncertainties of the kinetic parameters of purification processes on which manufacturers base their purity assignments, as well as the possible variations with time in a given product from a given source, such survey studies are indispensable. In fact, periodic surveys of a similar nature would provide vital nourishment to the proper continuity of the program since the flow of material on the market, being extremely restricted in time, is a constraint.

Tb has been found to be the most common and obstinate impurity. Our attempts to detect Tb in the $\sim 10^2$ ppm concentration in Y_2O_3 powder by ESR at liquid helium temperature were unsuccessful. Optical fluorescence methods were unsuccessful. Although emission spectroscopy has a detection limit of a few hundred ppm in Tb_4O_7, it became apparent that the color of the oxidized powder was a more sensitive index. The color of the undoped crystal is even more sensitive to the presence of this impurity, as it easily betrays a few ppm in the background.

Paralleling this survey study was the development of suitable purification procedures (anion and cation exchange methods) to provide sufficient flexibility for adaptation to the impurity spectrum of the best raw yttria available. A procedure based on an anion exchange method[2] was developed, and an eight-column purifier was constructed. The assembly, shown in Figure 1, consists of two separate units (four columns in parallel) which can be operated either in series or as two independent alternating units. The output capability is $\sim$ 100 g da^{-1}.

This anion exchange method has proved to be effective in the separation of lanthanides lighter than Tb. (The separation efficiency increases with decreasing atomic number.) The removal of heavier lanthanides has been accomplished by cation exchange. The results of studies on both of these purification methods are given in Appendix II[3].

For the maintenance of materials purity, some attention has been devoted to contamination pickup in the conversion of powder to crystal (boule). The parameters found to be most relevant are the furnace conditioning (age, moisture content, etc.) and the nature of the lining. The latter is associated to a certain extent with the problem of structural stability.

(2) Powder Technology

Another important and major phase in the advancement of crystal growth is the attainment of a more favorable heat balance. In the Verneuil growth of such highly refractory

---

2 J. P. Faris and J. W. Warton, Analytical Chemistry, 34, 1077 (1962).

3 Yb^{+3} and Dy^{+3} appear to be the most deleterious impurities in Y_2O_3:Nd^{+3} for the purpose of lasers. Such impurities will have to be classed accordingly in future surveys.

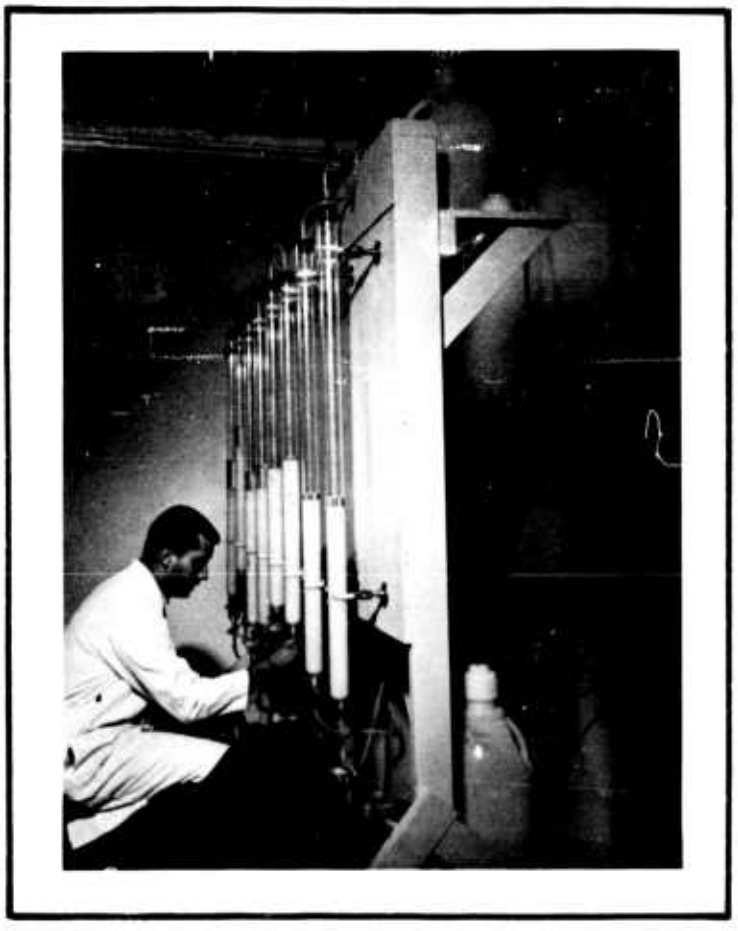

Figure 1

EIGHT-COLUMN ASSEMBLY FOR THE PURIFICATION OF YTTRIA BY ION EXCHANGE

oxides, the stringent control of powder flow is of prime importance and should not be underestimated. Material flow is linked to the maintenance of a steady state in heat balance throughout the growth process. The strict control of heat balance implies a rigid monitoring of heat sources and sinks. The powder stream is the main heat sink from the trajection region to the interfacial zone where growth occurs.

A phenomenological characterization of powder flowability was pursued by way of a study on the kinetics of packing. As expected, the packing behavior was found to be markedly dependent on the surface condition of the powder.

The working models subjected to this experimental study apply to the case where the mass of the powder remains constant with time in a sedimentation chamber. Pulsed sound is employed to study the kinetics of packing at a rate much faster than natural sedimentation. (The pulse repetition rate is characterized by a period much shorter than the natural relaxation time.) This provides a relative measure of z_p, the friction between powder particles. The observed behavior shows some similarity to "condensation". And the effect of surface conditioning on z_p is demonstrated with the use of an inert coat. Aging and/or moisturization of the powder also has a pronounced effect on flowability.

The results of our study on flowability are given in Appendix III.

(3) Verneuil Crystal Growth

During the early part of the study on provision of a more favorable heat balance, various fuel mixtures were

investigated and burners were redesigned and refabricated in-house. Boule diameter capability increased from ~ 1/8 inch to ~ 1/4 inch.

Typical boule sizes achieved within the first six months of the contract period are indicated by the monocrystal specimens shown in Figure 2. Such crystals were cut and polished at the ends. When viewed along the axis, the areas quite limited in extension appeared cloudy. This was apparently caused by powder cascading. In order to minimize the effect of such an excessive and erratic thermal loading of the flame, the growth rate was further reduced. Although this action enabled an improvement in crystal quality, it was evident that even further gains could be realized with the achievement and maintenance of a more appropriate heat balance.

A significant part of our third quarter activity was therefore devoted to the design, test, and assembly of an operational Verneuil apparatus incorporating an auxiliary burner. The system is shown in Figure 3. Auxiliary heat has a two-fold purpose. The first is to enable the scale-up in boule diameter by reducing radial thermal gradients in the furnace. The second is to provide on-the-spot annealing.

Scale-up was easily achieved. Figure 4 shows one of the early boules. (Fabricated $Y_2O_3:Nd^{+3}$ boules of an earlier vintage were included in the photograph for comparison purposes.)

Attainment of on-the-spot annealing, which is quite pertinent to crystal quality, has been thwarted by a structural instability of the assembly over the long period of exposure required[4]. Even CaO-stabilized zircona (a

---

[4] With the present capabilities on the level of heat balance, greater attention to powder flowability will be required to attain finer scale improvement in crystal quality.

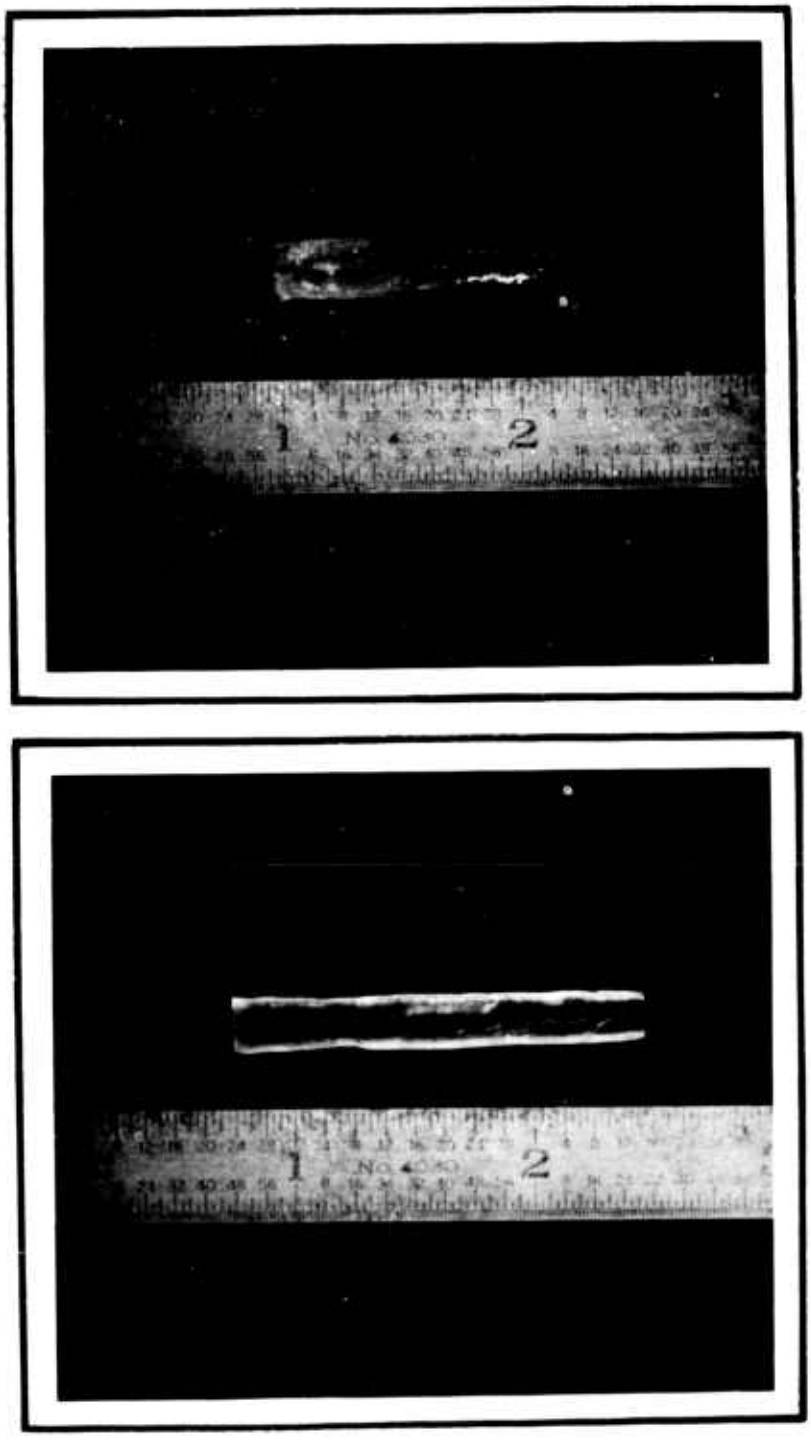

(a)

(b)

Figure 2

TYPICAL SIZE OF MONOCRYSTALS (UNCRACKED) OF DOPED YTTRIA GROWN BY FLAME FUSION

(a) $Y_2O_3:Sm^{+3}$

(b) $Y_2O_3:Nd^{+3}$

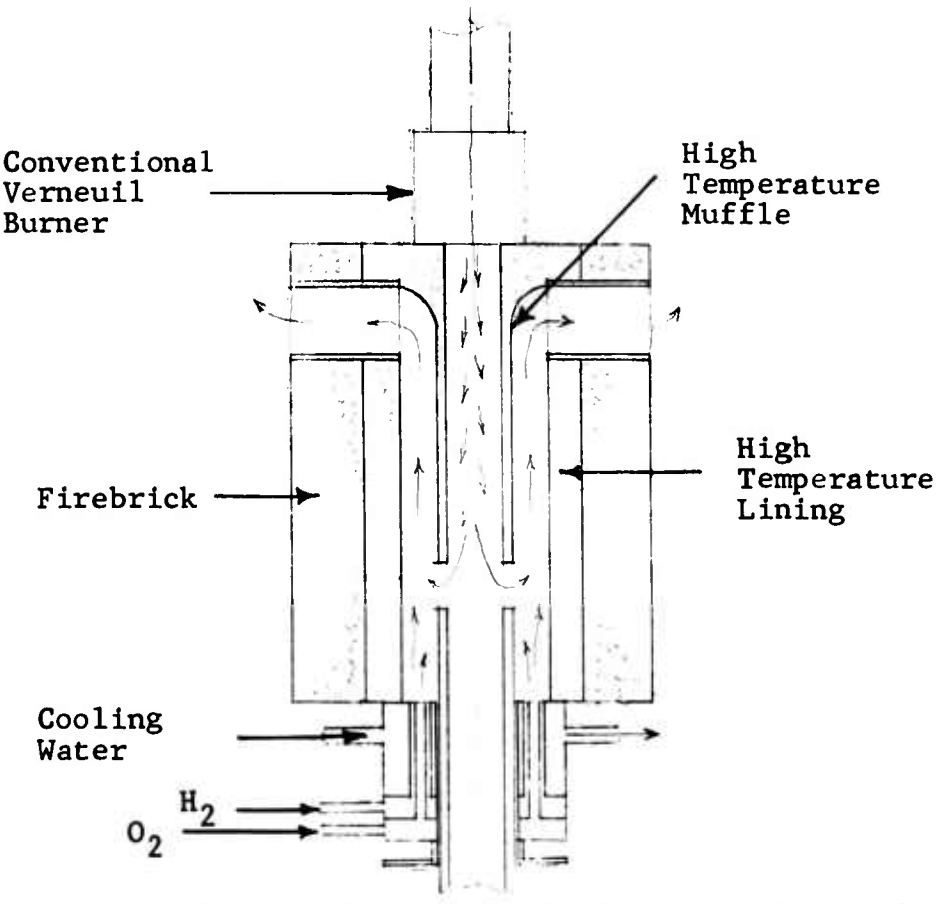

(a)

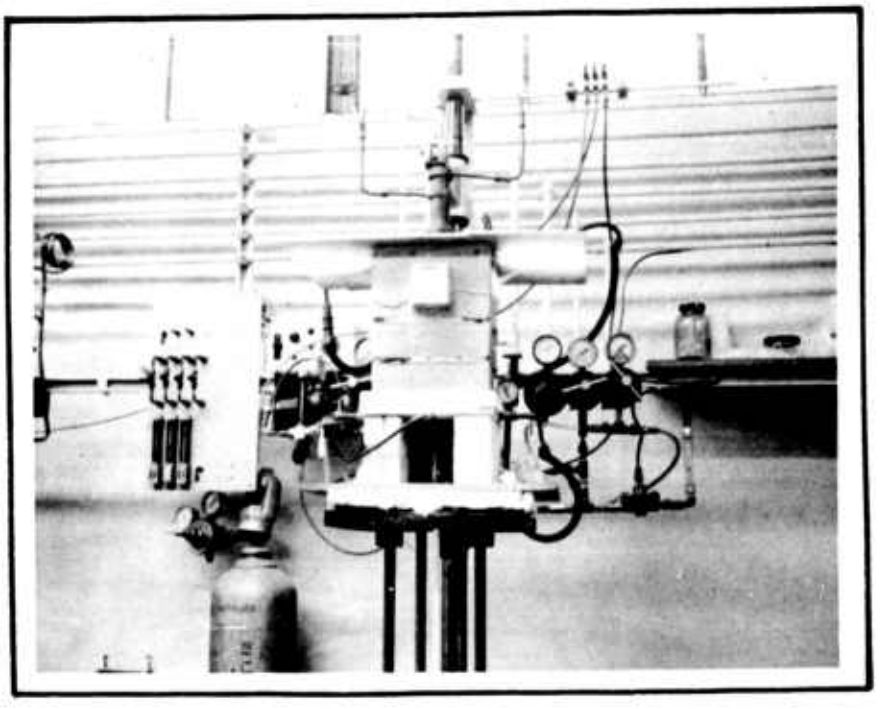

(b)

Figure 3

VERNEUIL APPARATUS FOR THE GROWTH OF LARGE MONOCRYSTALS OF Y_2O_3

(a) Schematics for the Double-Burner Configuration
(b) The entire assembly in operation

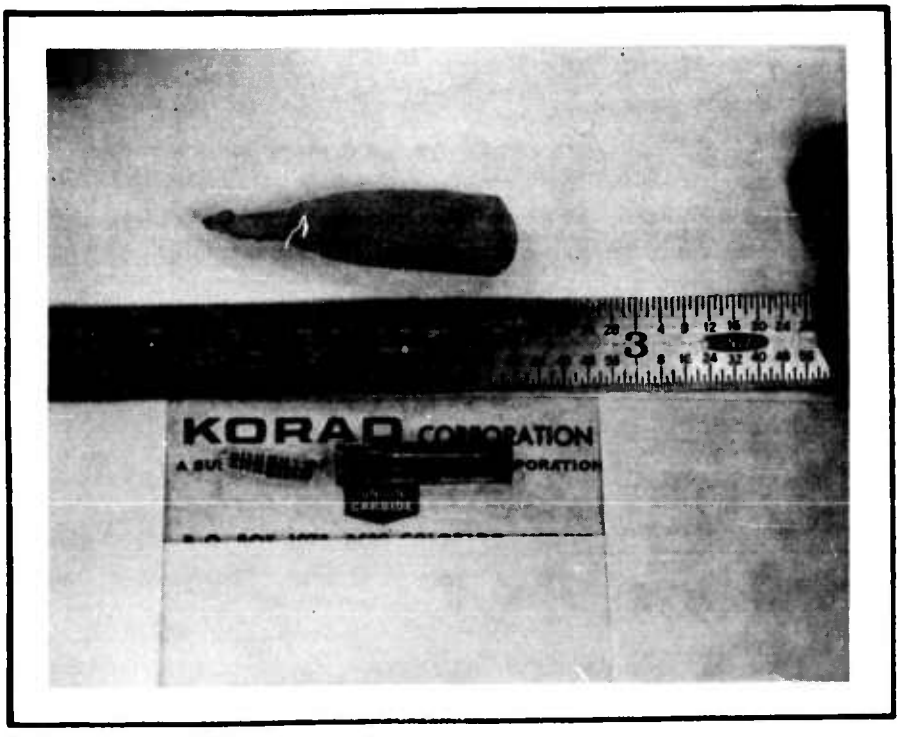

Figure 4

MONOCRYSTALS OF $Y_2O_3:Nd^{+3}$

Starting from the bottom left and proceeding counterclockwise typifies the scale-up in size between the first and third quarters of the contract period.

muffle material) has manifested an appreciable amount of creep over periods of ~ 10 hours at temperatures as low as 1950° C, which is still short of annealing. (Other muffle materials have been ordered and are currently being subjected to performance tests.)

Several $Y_2O_3:Sm^{+3}$ and $Y_2O_3:Tb^{+3}$ boules have been grown for spectroscopy and evaluation purposes, with emphasis being placed on low growth rates rather than on size scale-up. The surviving specimens were given the proper redox treatment prior to being submitted for evaluation.

In addition, a few small crystals of double-doped Y_2O_3 were grown for a preliminary study of sensitized fluorescence. The doping pairs of interest are (Nd, Ce), (Tb, Dy), and (Er, Tm).

(4) Crucible Method of Crystal Growth from the Pure Melt

The results of our studies on the thermal and chemical (corrosion) stabilities of candidate crucible materials have led us to believe that the problems encountered would be formidable for the Czochralski growth of Y_2O_3 (mp ~ 2450° C). As a consequence, no attempts will be made to crystal pull this material unless such is warranted by new developments in the pertinent technology.

B. Spectroscopy and Evaluation

Some effort was devoted to the laser evaluation of $Y_2O_3:Nd^{+3}$ during the first quarter of the contract period, using previous-generation crystals. Pulsed operation was obtained at room temperature in a crystal 7 mm in length with an input energy of 40 joules into a 1½-inch straight lamp. The output laser beam angle was relatively poor due to scattering from bubbles or cold powder sections in the crystal.

Laser testing of Y_2O_3 crystals was resumed early in the third quarter to provide a measure of the progress achieved in optical quality. The samples used were 2 to 3 mm in diameter and 1 to 2 cm in length. Typical of the results obtained was a room temperature threshold of 17 joules for a crystal one cm in length containing 1% Nd^{+3}. Normalizing to the same crystal length, CW-quality $CaWO_4:Nd^{+3}$ has a threshold of four joules in this same configuration. The concentration of the $CaWO_4:Nd^{+3}$, however, is approximately twice that of the $Y_2O_3:Nd^{+3}$. Therefore, the present status of $Y_2O_3:Nd^{+3}$ is that its threshold is about twice as high as the best quality $CaWO_4:Nd^{+3}$. This difference could arise from the fluorescent efficiency of the laser line, from absorbing impurities (e.g., Yb^{+3} or Dy^{+3}) that are present in the host material, or from optical quality (e.g., scattering or walk-off losses caused by index of refraction inhomogeneities).

A comparison of the fluorescence intensities of $CaWO_4:Nd^{+3}$ and $Y_2O_3:Nd^{+3}$ indicates that the fluorescent efficiency of emission at the laser wavelength under continuous tungsten lamp illumination is approximately the same in both materials. The difference in threshold probably arises from either poor optical quality or impurities. Our calculations show that impurity (e.g., Dy) levels lower than that presently detectable by emission spectroscopy could cause difficulties. An investigation of the optical quality is currently being made using Twyman-Green interferometry. Preliminary results indicate on the order of one fringe per mm per cm of length.

The fluorescence spectra in the visible of $Y_2O_3:Tb^{+3}$ has been taken at room temperature and at 77° K. The results are shown in Figures 5 and 6. Fluorescent lifetime of the groups near 4900 Å, 5900 Å, and 6200 Å was 1.6 msec. The lifetime of the 5500 Å group was 2.3 msec. The linewidth of the principal fluorescent line at 5430 Å was approximately 2.5 Å.

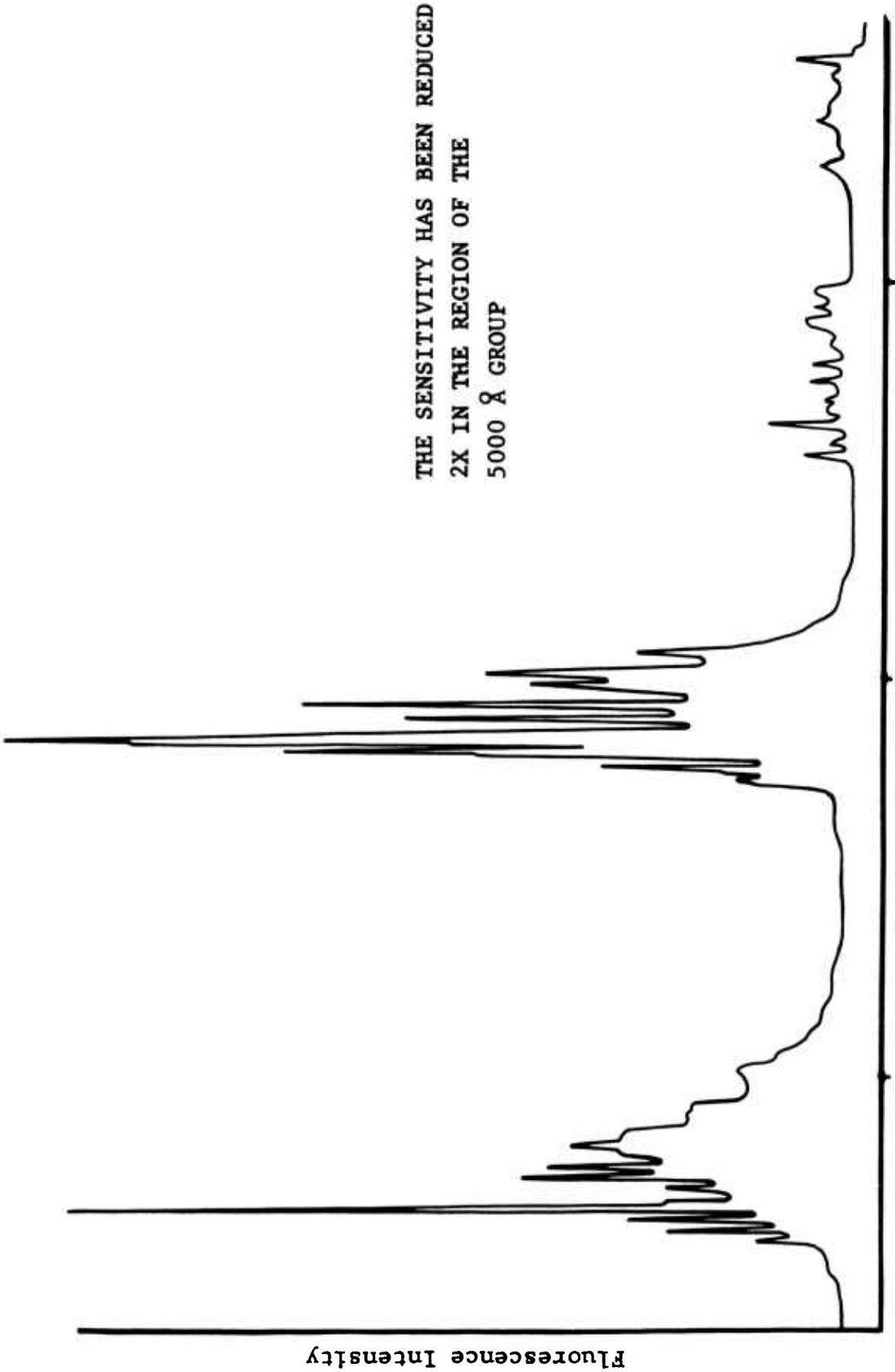

Figure 5

FLUORESCENCE SPECTRUM OF $Y_2O_3:Tb^{+3}$ AT 300^oK

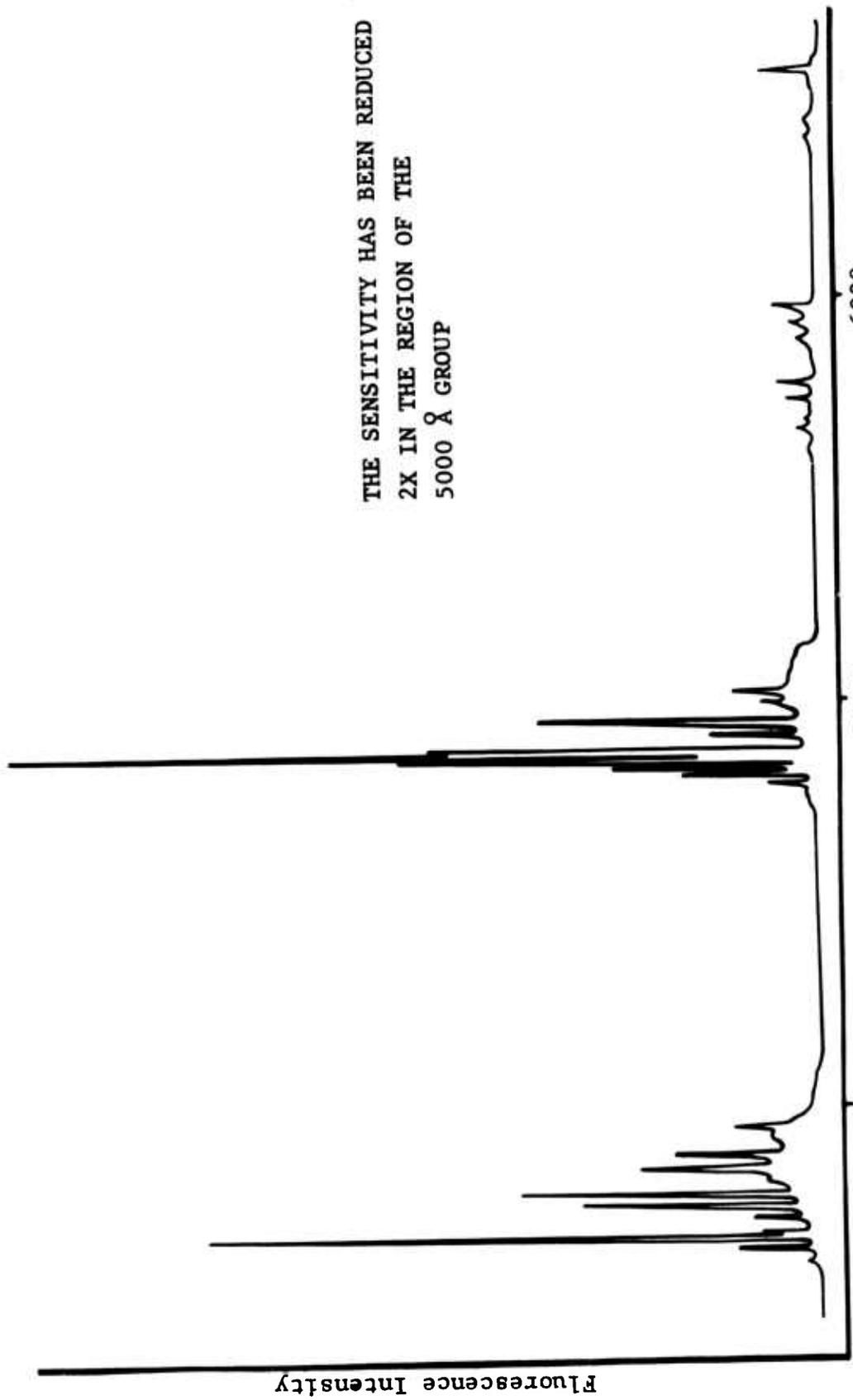

Figure 6

FLUORESCENCE SPECTRUM OF $Y_2O_3:Tb^{+3}$ AT 77° K

Fluorescent lifetime vs concentration has been measured in $Y_2O_3:Sm^{+3}$ crystals. The lifetimes varied from 0.2 msec to 1.0 msec over a concentration range of from one-half to five percent.

Preliminary evaluation of Y_2O_3 crystals containing Er^{+3} and Tm^{+3} has been started. The presence of Er^{+3} is known to enhance the 1.9 micron fluorescence of Tm^{+3} in $CaMoO_4$. A greater effect should be attainable in Y_2O_3, where larger concentrations of Er^{+3} can be incorporated. The fluorescence spectrum of $Y_2O_3:Tm^{+3}$ (one-half percent Tm^{+3} concentration) at 77^{o} K in the 1.9 micron region is shown in Figure 7. A few samples of $Y_2O_3:Tm^{+3}$ containing 10% Er^{+3} have been grown which show that an enhancement of the Tm^{+3} emission is indeed obtained. Our preliminary measurements indicate an enhancement of at least tenfold under tungsten illumination.

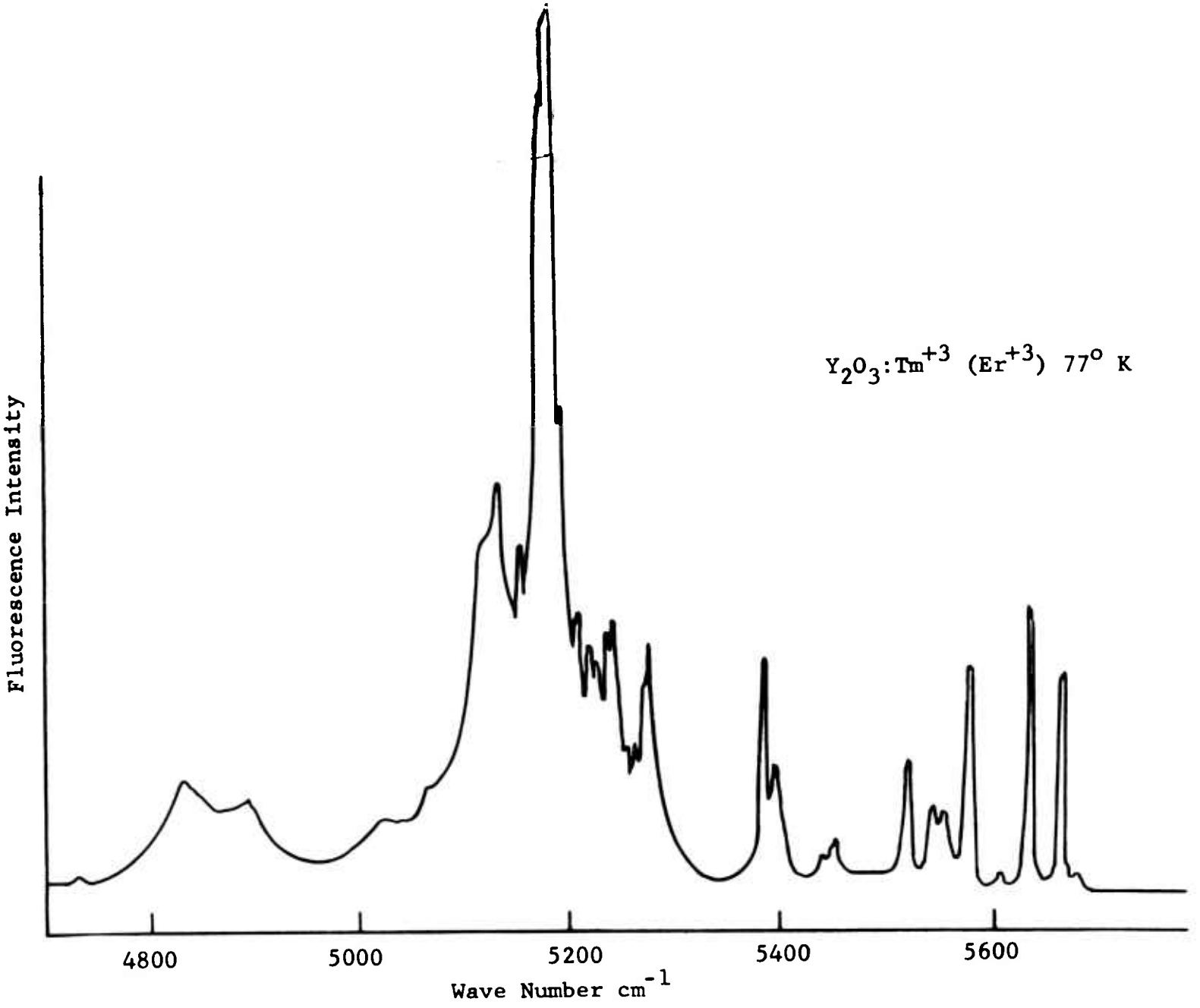

Figure 7

FLUORESCENCE SPECTRUM OF $Y_2O_3:Tm^{+3}$ AT 77° K

Section 3
BINARY HOST OXIDE - $LaAlO_3$ and $YAlO_3$

A. Synthesis and Crystal Growth

When the Final Report covering the preceding contract was written, the foremost barrier to an understanding of the crystal growth behavior of binary oxides was stoichiometry. This feature alone clouded the resolution of vital issues. Crystal products exhibited a wide variation of behavior -- to the point that property measurements were often feared to be meaningless, since they were suspected of being dependent upon the particular history of the material in question.

Color centers were affected by deviations from stoichiometry as well as background impurities. And these centers, in turn, were linked to crystal stability. The stability of monocrystals ranged from an ability to remain intact from the time of their growth to the present, or crumbled to a dense powder within hours of their growth. There was no first-order crystal phase transition reported for either the microcrystalline powder or the macrocrystal for a reasonable range of values in pressure and temperature. And, as would quite naturally be expected, our measurements showed no change in chemical composition or in crystal structure either before or after deterioration.

The pyrolytic methods for the preparation of powder feed (flame fusion), which had been used so successfully for the unary hosts, were found to be quite inadequate for the binary oxides from the standpoint of stoichiometry[5]. As a consequence, the study of congruency behavior at melting was ill-defined and the applicability of pure melt methods was a shaky assumption, particularly in the case of $YAlO_3$.

---

5 Analytical methods were unreliable guides because the attainable precision fell quite short of tolerable deviations from stoichiometry.

Our first objective at the inception of the present contract was therefore clear -- to obtain a truly stoichiometric feed. (This is also referred to as a one-phase binary oxide.) Once this had been achieved, the next task would be the establishment of kinetic congruence[6].

The test adopted, which is the fastest but suffers somewhat in sensitivity, was to determine the crystal structure invariance before and after melting[7]. If the material passed this stage, then three phases could be carried out simultaneously. The first would involve preliminary flame fusion work in order to provide specimens which were better than those previously employed, enabling a check on the earlier spectroscopy and optical evaluation findings. The second would be a study of powder technology directed toward improved flowability which is invariably required in the finer scale improvement of crystal quality. The third phase would be the conduct of corrosion studies for the selection of an appropriate crucible as part of a feasibility study on the Czochralski (crystal pull) method.

(1) Chemistry of Materials

To obtain a truly stoichiometric feed requires a determination of the operating conditions under which the stable phase (thermodynamically) carries the composition desired.

---

6 There is no phase diagram information readily available which establishes the thermodynamic congruence of $LaAlO_3$ or $YAlO_3$. Thermodynamic congruence is a necessary, but not sufficient, condition for kinetic congruence. Kinetic congruence is more pertinent to (and is dependent upon) the process of crystal growth.

7 If this invariance of crystal structure persists, independent of the time interval through which the material is kept molten, then an operational proof for kinetic congruence is constituted. The time interval chosen should be equal to or greater than that which is characteristic of the process in question (viz., crystal growth). Allowance should be made for the fact that the nature of the atmosphere often affects the question of kinetic congruence.

In addition, a process is chosen that will effect a realistic kinetics of formation. Since the phases desired are stable at high temperatures, the synthesis can be carried out in nonaqueous solvents which are capable of accomodating such operating conditions. Well-known physical (phase) transitions have served as a rough index for the kinetics of these preparations.

The stoichiometric feed for $LaAlO_3$ was achieved during the first quarter of this contract period. By the second quarter there was evidence of congruent behavior at the melting point for La:Al = 1:1 and incongruent behavior for the 3:5. Parallel runs indicated the opposite case for Y:Al (i.e., incongruent behavior for the 1:1 and congruent behavior for the 3:5). Further work on $YAlO_3$ was consequently abandoned in favor of a greater concentration of effort on $LaAlO_3$.

As mentioned earlier, the test for kinetic congruence (powder X-ray diffraction) lacks in sensitivity. The final proof lies in the actual crystal growth of the materials. X-ray diffraction is, however, a useful test as an adjunct to powder synthesis and serves to eliminate those procedures where gross differences in the products are observable.

We have now developed a number of methods for the preparation of a one-phase $LaAlO_3$ powder. One such process is briefly described here to serve as a typical example. The pH curve shown in Figure 8 indicates the successive precipitation of the hydroxides in an equimolar solution of lanthanum and aluminum nitrates. An intimate mechanical mixture results from this method. The residue obtained from the suspension which is stirred overnight at room temperature shows (X-ray) no $LaAlO_3$ phase. If the last processing step is repeated, however, with the suspension kept at 85° C instead of room temperature, the conversion

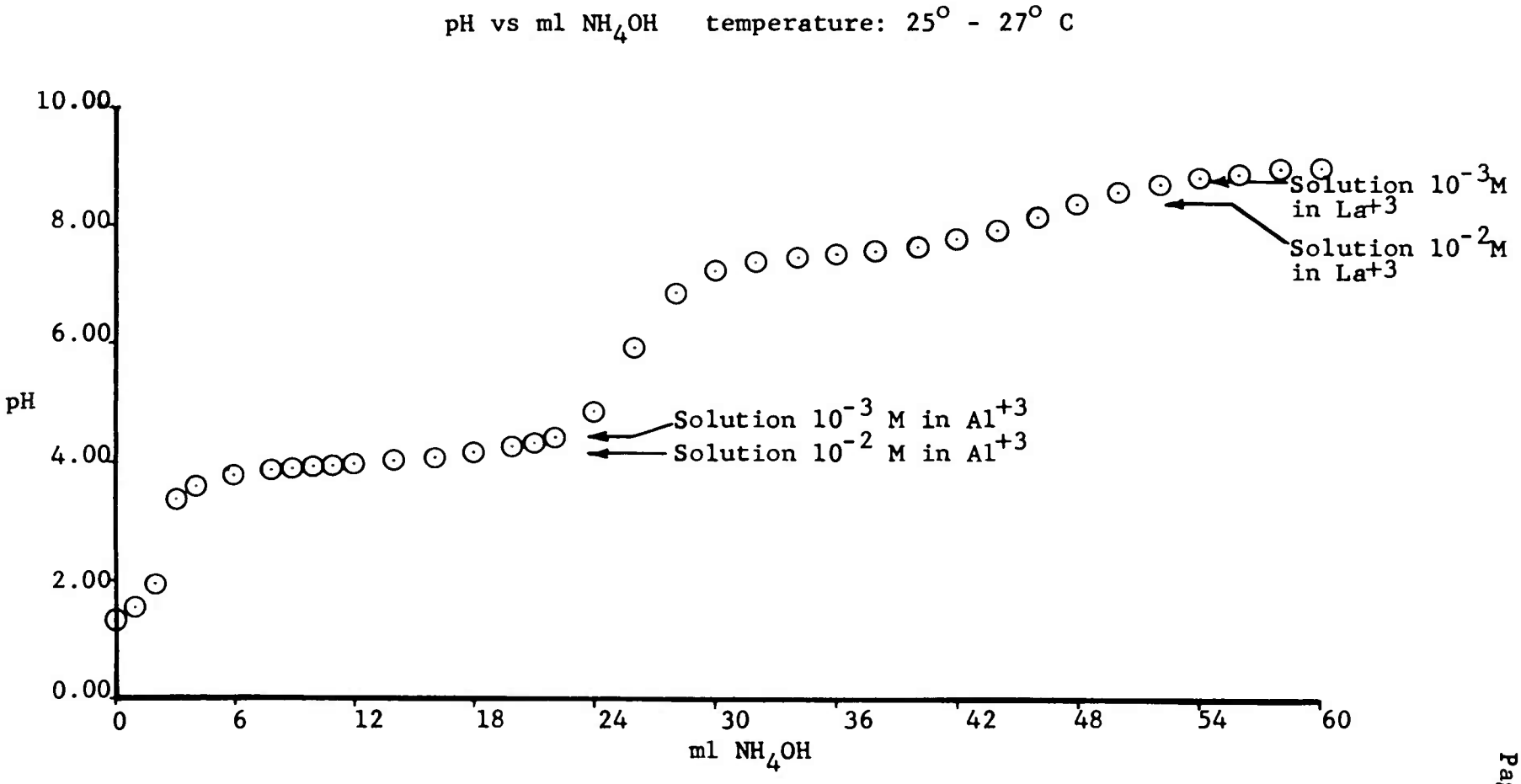

Figure 8

SUCCESSIVE PRECIPITATION OF THE METAL HYDROXIDES FROM AN EQUIMOLAR SOLUTION OF LANTHANUM AND ALUMINUM NITRATES

to the $LaAlO_3$ phase is found to be complete. The concentration of cation remaining in the solution, as shown in Figure 8, was calculated from the solubility product constant. No interaction between the two components and the complete ionization was assumed in these dilute solutions.

(2) Powder Technology

Once the synthesis recipe for a stoichiometric powder has been established, a further manipulation of the processing parameters is required in order to achieve the physical texture called for by Verneuil crystal growth[8]. This involves a laborious search. The guide employed at present is a flow characterization of the product (see Appendix III).

Relevant results are often rendered ambiguous by unforeseen parameters which are not controlled in the storage of the powder. At times the change in flowability under short storage can spell the difference between the case where a crystal is easily grown and that where even mere nucleation is impossible to achieve.

We can sum up the present status of powder technology for $LaAlO_3$ in terms of control and reproducibility. Both features of processing appear to have been achieved for stoichiometry -- but not for flowability. With powder samples in which both the stoichiometry and flowability characteristics are attained to a relatively satisfactory degree, boules of $LaAlO_3$ are easily grown with a quality that is distinctly superior to those obtained in the past.

(3) Verneuil Crystal Growth

With the low level of growth rates employed, it is estimated that the limited melt of the Verneuil method is replenished in a period of from five to ten minutes.

---

8 This step is not required in the Czochralski method of crystal growth.

It can therefore be appreciated that a binary oxide powder feed which is even slightly off stoichiometry can easily (within the first hour of operation) attain a melt composition whereby the desired phase cannot crystallize out any more. A feed may be stoichiometric, the crystal phase may be thermodynamically congruent, and yet behavior can be kinetically incongruent. This could be due to dissociation in the melt, coupled with an appreciable vapor pressure of the components. The case is exceptional where vaporization losses leave the melt composition unchanged[9].

The successful Verneuil growth of $LaAlO_3$ crystals closely followed the first demonstrations of congruence. Typical specimens of $LaAlO_3:Nd^{+3}$ are shown in Figure 9. The clarity of these specimens is so striking that, when illuminated by transmission, lines of cold powder arising from infrequent cascades are easily discernible.

There does, however, appear to be some crystal quality problem associated with the direction of spontaneous growth. Two approaches to solution of this problem are under study. The first is to attempt an oriented (as opposed to spontaneous) nucleation to determine if the difficulty is intrinsic to the orientation or to the system. The second approach is to examine the stabilizing effect of A and/or B ions in $(La_{1-\alpha}A_{\alpha})AlO_3$ and $La(Al_{1-\beta}B_{\beta})O_3$. The suggested stabilizers are A = Bi and B = Sc.

(4) Crucible Method of Crystal Growth from the Pure Melt

The most distinguishing feature of the Verneuil method of crystal growth is an extremely limited melt. Since this is bounded only on one side by an interface region where the crystal growth takes place, both the problems of heat

9 If such a case is obtained, it is most likely a vaporization of the molecular species of the binary material.

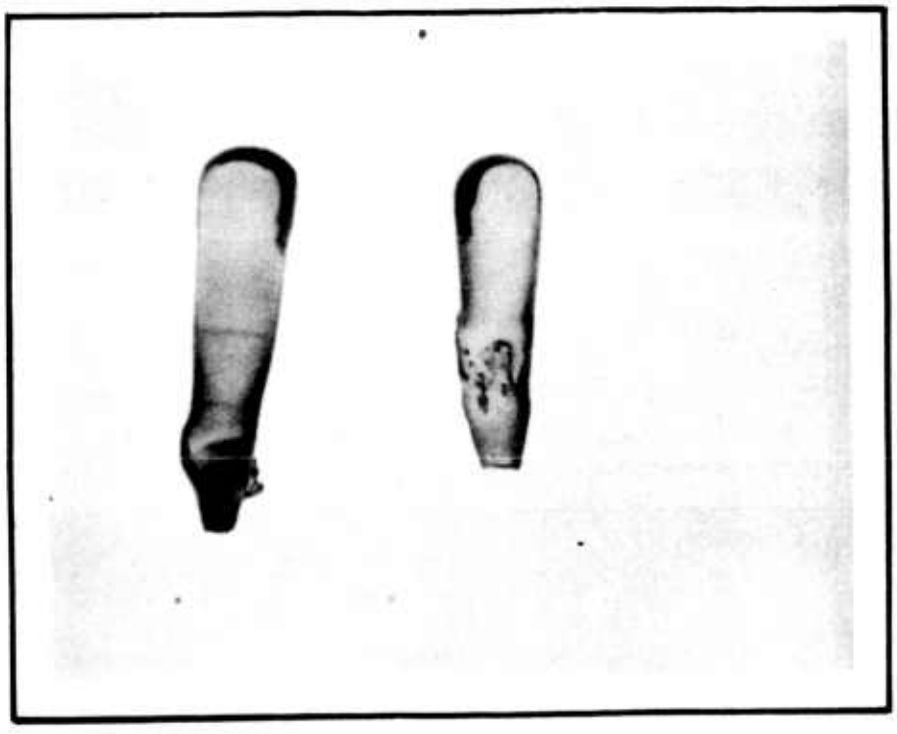

Figure 9

TYPICAL SPECIMENS OF $LaAlO_3:Nd^{+3}$ BOULES

Scale is 4X. Illuminated by transmission. Clarity of specimen shows presence of a cold layer in the boule on the left hand side.

control and those of material flow are much more exacting than in crucible growth methods. The Czochralski (an example of a pure melt crucible method) deals with a melt size $\sim 10^3$ times larger and can therefore buffer the effects of a short-lived perturbation in the heat balance, as well as a drift in composition. Either of these would be disastrous to the Verneuil or any other zone method of crystal growth.

The problem of powder flowability is germane to the Verneuil method -- but not to the Czochralski. There are, therefore, four major advantages to a trade-off of a Czochralski in place of a Verneuil:

- a much simpler chemistry of materials for the binary,
- elimination of the whole manifold of problems on powder technology,
- a large thermal inertia of melt to buffer the thermal fluctuations (very important to crystal quality), and
- a large mass of melt to buffer drift in composition through the range which allows crystallization of the phase with the desired stoichiometry.

This last item loses its significance, however, in the case where both sides of the given composition of the binary are bridged by solid solutions.

We next consider the disadvantages which would follow such a trade-off. The most important one stems from the large melt -- the feature on which all of the advantages listed above are based. A crucible is required to contain

such a large phase (melt). Hence, in the search for a suitable crucible material, we have essentially traded the physical chemistry problems of the Verneuil for the corrosion chemistry problems of the Czochralski.

A significant rating on corrosion resistance for our purposes should be derived from a temperature-time (exposure) figure of merit. The temperature adopted should be that which is the melting point of the material in question. And the time rating for exposure should be determined at such temperature. The behavior should then be extrapolated to a time scale which is commensurate with that required for crystal growth.

We have endeavored to carry out this rating procedure for the case of $LaAlO_3$, undoped microcrystalline powder. Argon was the atmosphere provided in most of these tests. The temperature recorded is the reading taken from the pyrometer (not corrected for emissivity). The actual exposure at the "melting" or "reaction" temperature ranges from 10 to 15 minutes.

One of the most refractory candidates comes from Group IV, viz., C (mp > 3500° C). The impracticality of carbon as a crucible material for $LaAlO_3$ can be predicted on the basis of corrosion findings on the components. Fairly rapid reaction with C is observed (in an He atmosphere) at ~ 1950° C for Al_2O_3 and at ~ 2200° C for La_2O_3. $LaAlO_3$ liquifies at ~ 2050° C, reacting quite quickly with carbon.

The refractory metal candidate taken from Group V is Ta (mp, 2996° C). Pyrometer readings at "melting" indicate ~ 1950° C. A fairly energetic reaction is manifested while at this temperature. When the melt has cooled down, it is evident that the composition is changed (the melt is firmly cemented to the foil). No crystal phase of $LaAlO_3$ is seen under the microscope. These results are shown in Figure 10.

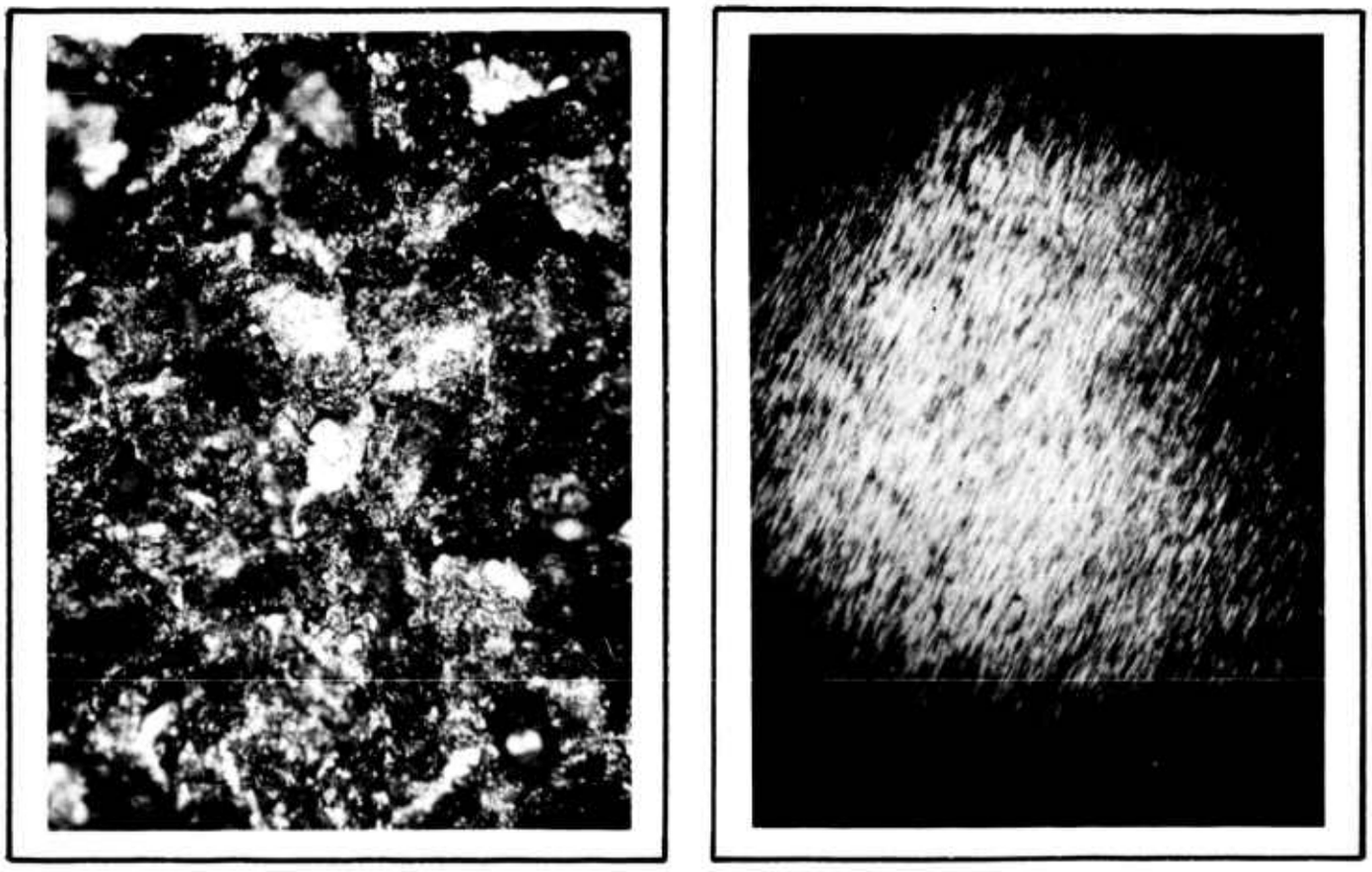

(a) (b)

Figure 10

MELTING OF $LaAlO_3$ IN Ta (0.002 INCH FOIL)

(a) Melt reacted with foil (X80)

(b) Ta foil before use (X80)

The candidates examined from Group VI were Mo (mp, 2620° C) and W (mp, 3370° C). In the case of Mo, reaction was in evidence at the melting point (pyrometer reading was ~ 1955° C). When the melt cools down, $LaAlO_3$ crystals are easily seen. The cooled melt was discolored, to a charcoal grey. Although the melt dislodged easily, the foil surface was badly etched and cracked. The results are shown in Figure 11. Note, in Figure 11(a), the fine network which arises from crystallization of the metal by thermal cycling (may have been catalyzed by melt). The behavior of W parallels that of Mo, except that much less reactivity is noted. The pryometer reading at the melting point was, again, ~ 1955° C. $LaAlO_3$ crystals are easily manifested in the cooled melt. The cooled melt pries off easily, leaving a shiny surface. The effect of etching is readily observable, however, for this short exposure time. These results are shown in Figure 12.

For Group VII, the refractory candidate chosen was Re (mp, 3167° C). No evidence of corrosion was evidenced with $LaAlO_3$. The pyrometer reading for melting was ~ 1950° C, and the cooled melt was easily dislodged from the foil which remained shiny, as shown in Figure 13. Although thermal cycling caused crystallization of the metal (compare (a) and (b) of Figure 13), the foil remained very pliable.

The refractory candidate chosen from Group VIII was Ir (mp, 2454° C). The results of a corrosion test with molten $LaAlO_3$ are shown in Figure 14. The pyrometer reading for melting was ~ 1940° C. As seen in Figure 14(b), the metal does not fabricate well because of its brittle nature. This defect becomes even more exaggerated after thermal cycling, Figure 14(a), because of crystallization of the metal. A mild etching effect from the melt can also be seen. The cooled melt was difficult to dislodge, probably due to keying in the cracks as well as grain boundaries.

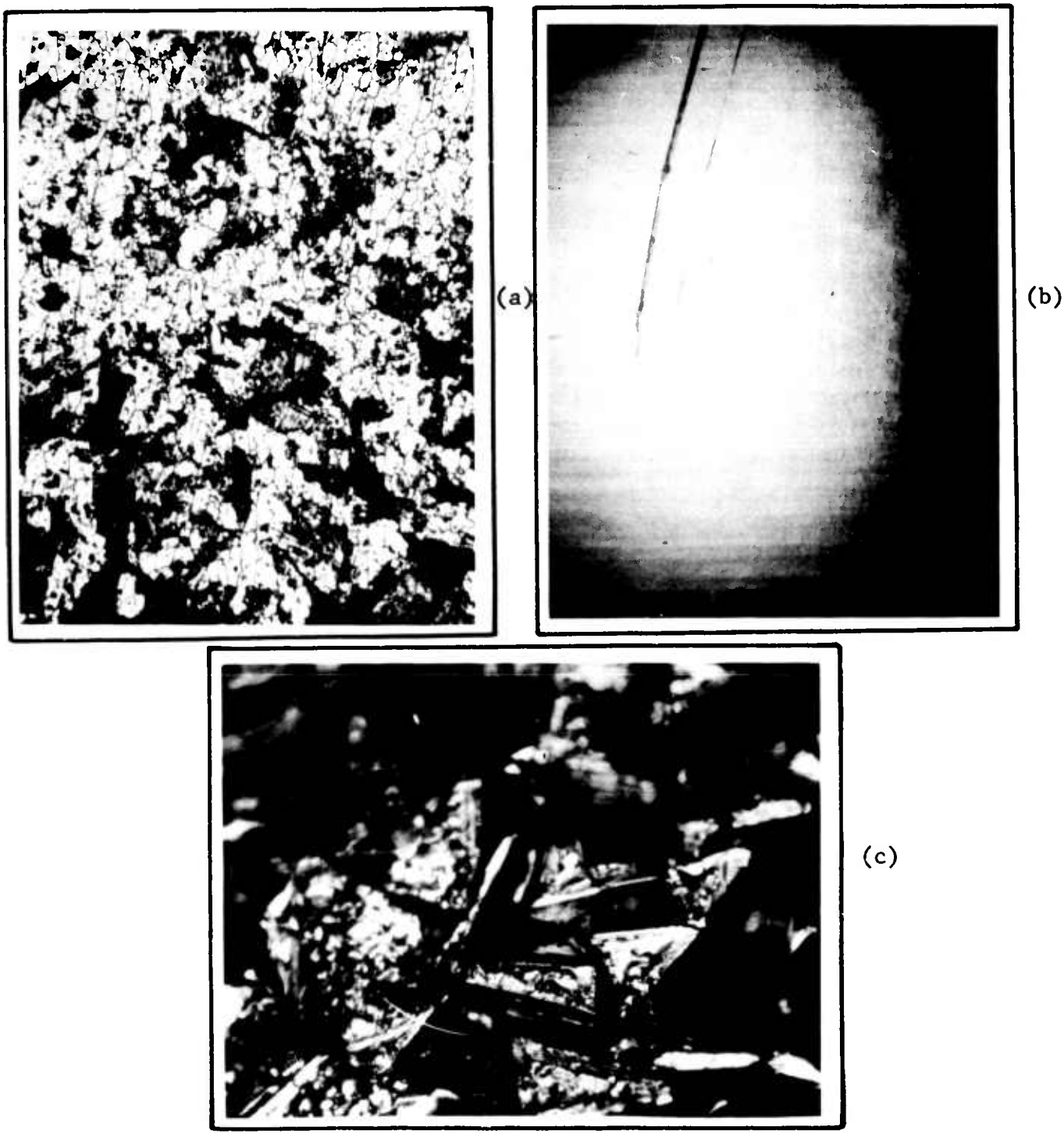

Figure 11

MELTING OF $LaAlO_3$ IN Mo (0.005 INCH FOIL)

(a) Foil surface after melting (X 80)
(b) Foil surface before melting (X80)
(c) $LaAlO_3$ crystals from the melt on Mo foil (X80)

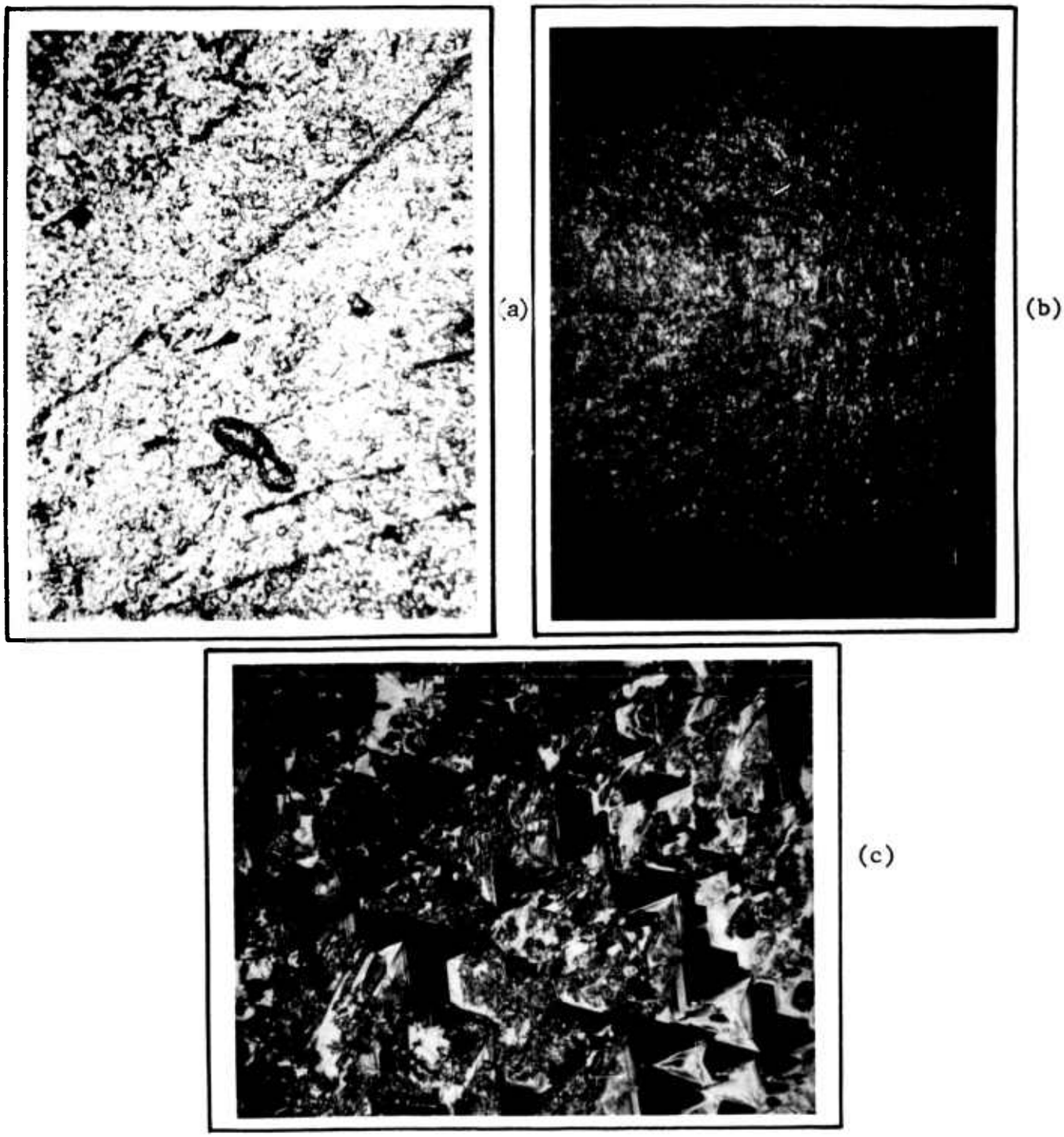

Figure 12

MELTING OF $LaAlO_3$ IN W (0.005 INCH FOIL)

(a) Foil surface after melting (X 80)
(b) Foil surface before melting (X80)
(c) $LaAlO_3$ crystals from the melt on W foil (X80)

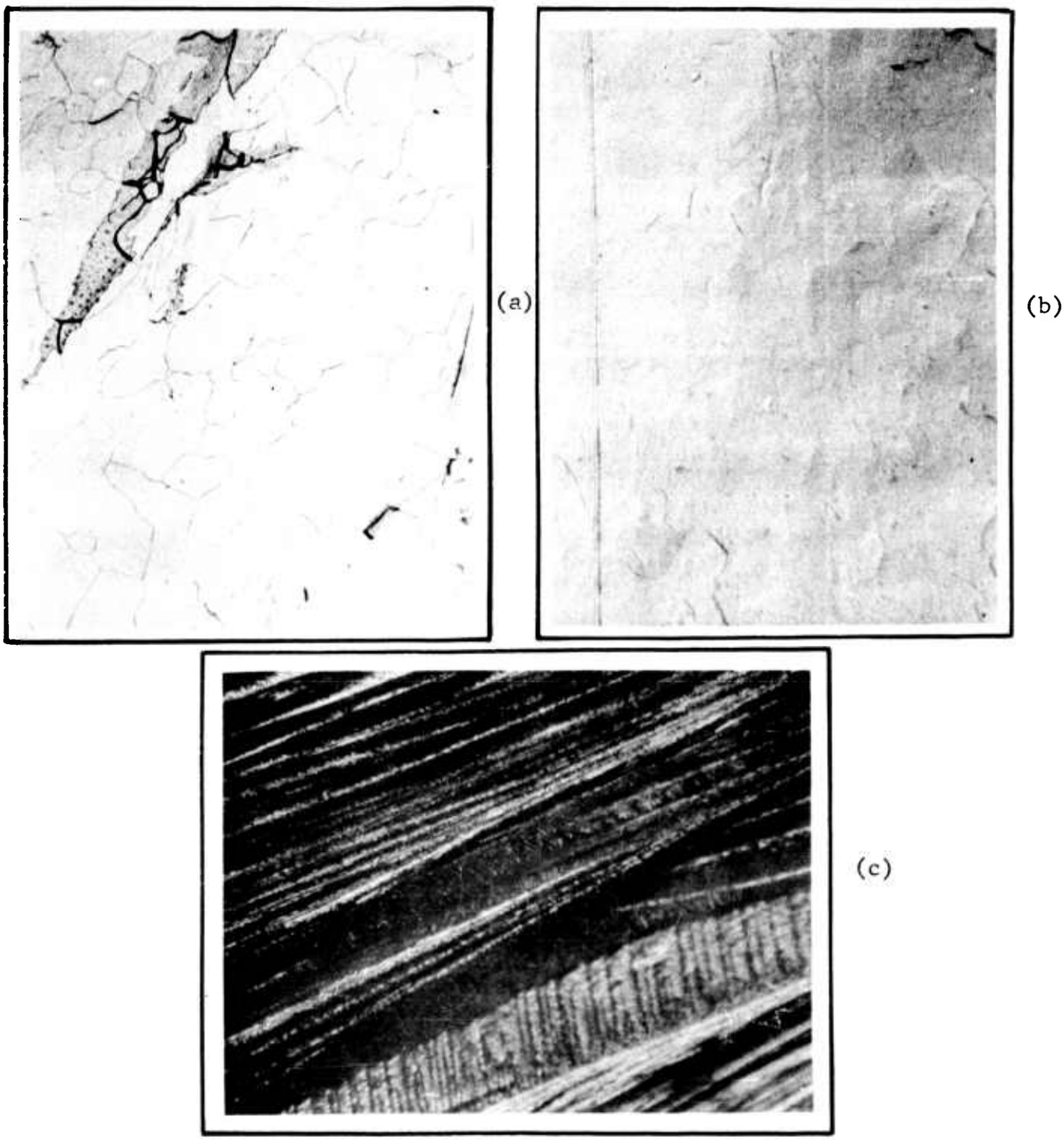

Figure 13

MELTING OF $LaAlO_3$ IN Re (0.002 INCH FOIL)

(a) Foil surface after melting (X 80)
(b) Foil surface before melting (X80)
(c) $LaAlO_3$ melt cooled rapidly on Re foil (X80)

(a)

(b)

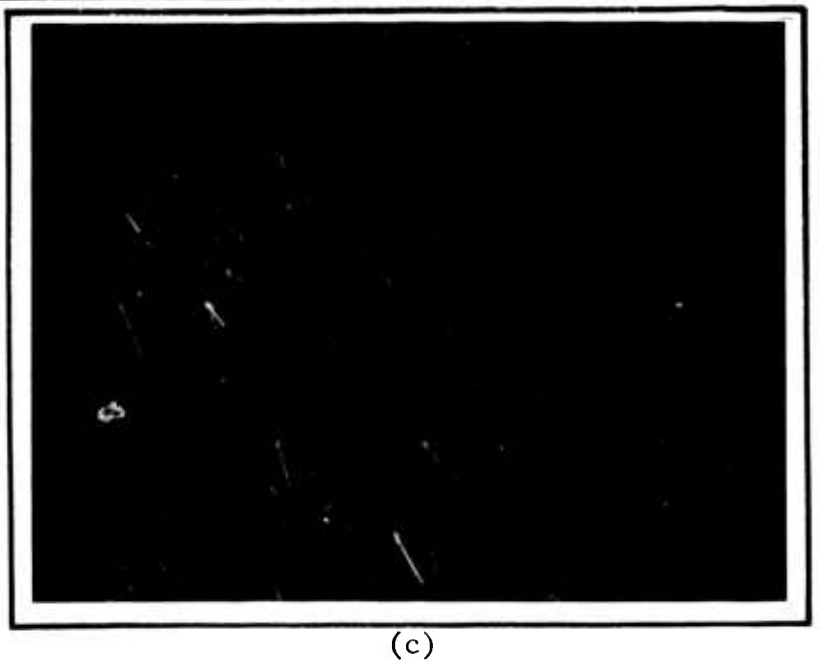

(c)

Figure 14

MELTING OF $LaAlO_3$ IN Ir (0.0015 INCH FOIL)

(a) Foil surface after melting (X 80)
(b) Foil surface before melting (X80)
(c) $LaAlO_3$ cooled melt on Ir foil showing crystals (X80)

It is concluded that where there is very little or no reaction, true melting is observed with a pyrometer reading appearing consistently at ~ 1950° C. The three least reactive candidates (in the order of decreasing resistance to corrosion) are Re > W > Ir. We also conclude from these observations that Re is the only elemental material in the entire collection of refractory metals tested that stands a fair chance for actual crystal growth runs (~ 10 hr exposure vs 0.2 hr in the corrosion test). However, the reduction in reactivity by alloying should not be overlooked (e.g., W - Re).

B. Spectroscopy and Evaluation

Powder X-ray studies were carried out on $LaAlO_3$ powder prepared under the non-aqueous solvent process, and comparisons were made with the powder used in previous crystal growth attempts. As seen in the powder X-ray photograph of Figure 15(a), a mixture of structures is clearly exhibited. The much simpler pattern shown in Figure 15(b) corresponds to stoichiometric $LaAlO_3$ with no other structures present.

An uncracked crystal of $LaAlO_3$, very lightly doped with Cr^{+3}, and grown from the stoichiometric powder, was investigated. The shape of the spots in Laue X-ray studies of this crystal, grown along the (111) direction, indicates relatively good crystal quality. Debye rings are discernible, however, which probably arise from undissolved powder. Some strain is evidenced by examination through crossed polaroids. The fluorescence spectrum shows an extra line about 15 Å to the long wavelength side of R_1 and R_2 which is not attributable to pairs of Cr^{+3} ions since the crystal is very dilute. This line decreased in intensity relative to R_1 and R_2 after prolonged UV irradiation which caused a brown coloration to develop. The laser pumping cross-sections were determined to be about 4×10^{-21} cm^2 in the green band and 4×10^{-20} cm^2 in the blue-violet.

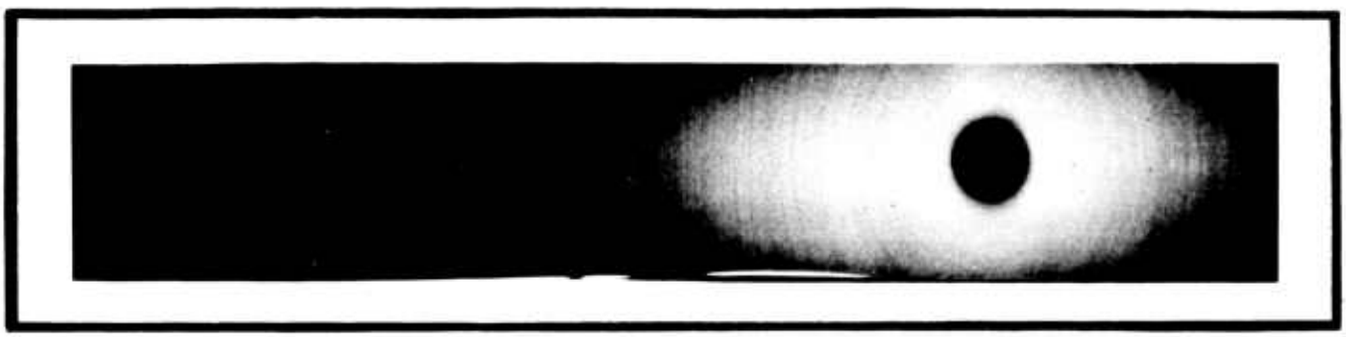

(a)

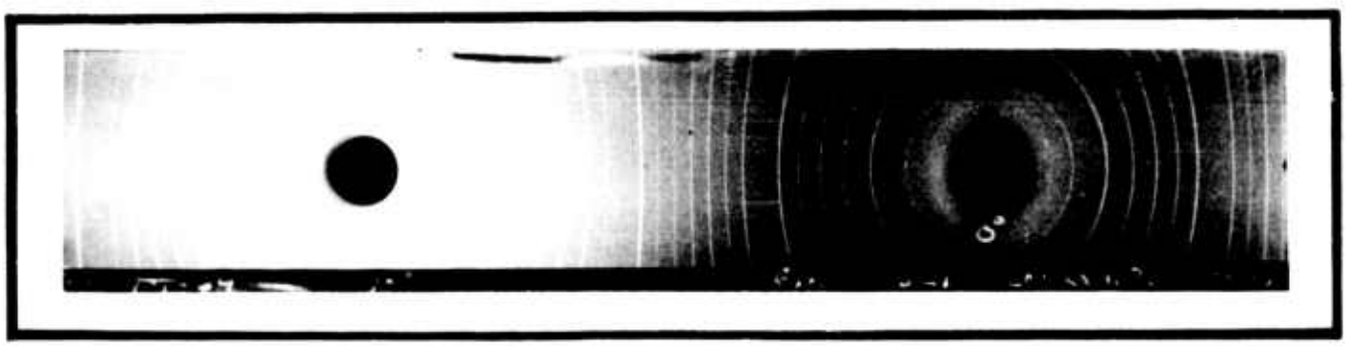

(b)

Figure 15

X-RAY POWDER PHOTOGRAPHS OF $LaAlO_3$

(a) Mixed (b) Stoichiometric

Some of the $LaAlO_3:Nd^{+3}$ samples which appeared to be very clean crystals on the outside proved to have an internal scattering effect when optical windows were polished on the sides of the boules. When viewed under a low-powered microscope, scattered light gives the crystals a cross-hatched appearance. This effect is currently under investigation.

PLANS FOR NEXT REPORT PERIOD

Crystal quality improvement studies on Y_2O_3 will be continued during the next report period. The growth of mixed crystals (solid solution) with this host material will be carried out, using both single and double-doping, in support of findings from the evaluation.

Stabilization studies in the crystal growth of $LaAlO_3$ will be conducted, as well as powder synthesis with respect to control and reproducibility of powder flow. Corrosion investigations will be continued in support of the feasibility study of the Czochralski method of crystal growth.

APPENDIX I

Survey Study of Sources of Raw Yttria for Crystal Growth

SURVEY STUDY OF SOURCES OF RAW YTTRIA FOR CRYSTAL GROWTH

by

H. Kimura and J. Tarris

A market survey for a satisfactory Y_2O_3 source was initiated as a result of a brown discoloration which appeared in boules grown from American Potash 4-9 purity powder (LU 1111, Code 1116). The alkaline earths were found to be somewhat low to account for what was observed. The cause was eventually traced to the presence of Tb_4O_7.

It then became evident that, in the purchase of raw Y_2O_3, the RE-purity (i.e., purity with respect to rare earths) may at times be secondary in importance to the spectrum of rare earth impurities. This is very pertinent to the economics of in-house purification.

In the present survey study, the emphasis of the search was for a powder source with a low Tb_4O_7 background. Seven manufacturers responded and provided powder samples of various purity ratings. The results of the analyses by emission spectrograph are collected in Table I-1.

The standard curve for Tb_4O_7 in Y_2O_3 was extended from 200 to 100 ppm. ND means the line is completely absent, in which case the concentration of Tb_4O_7 is < 80 ppm. At times, due to the high content of Tb_4O_7, it was felt to be unnecessary to pursue the analysis further. (Note the case of Varlacoid in Table I-1.)

For Dy_2O_3, ND means < 400 ppm when Er_2O_3 is present and < 10 ppm otherwise. The standard curve for Er_2O_3 was extended to 50 ppm. However, ND for Er_2O_3 is most likely < 10 ppm. For Yb_2O_3, the standard curve was constructed down to 10 ppm where the

	American Potash	Fair-mount	Vitro		Michigan Chemical			McKay		Research Organic		Varla-coid	Zucker-man (c)
	4-9	3-9	3-9	4-9	3-9	4-9	5-9	3-9	4-9	3-9	4-9	3-9	5-9
Ca	(a)	180	150	82	500	59	620	54	450	960	45	(a)	290
Mg	(a)	19	15	27	15	12	23	25	43	35	39	(a)	40
Tb_4O_7	150	ND	ND	ND	ND	ND	ND	ND	ND	ND	ND	150	ND
Dy_2O_3	ND	980	1200	1300	1100	130	ND	90	ND	1100	ND	(a)	ND
Er_2O_3	150	140	ND	ND	ND	ND	32	ND	ND	50	ND	(a)	ND
Yb_2O_3	10	12	1200	<10	ND	ND	ND	26	56	320	<10	(a)	ND
RE-Purity	99.97	99.9	99.8	99.9	99.9	99.99	99.997	99.99	99.997	99.9	99.9998	(a)	110.
$ Lb^{-1}	75.	60.	52.	60.	52.	60.	220.	(b)	(b)	65.	75.	52.	90.

(a) Not Determined.

(b) The price available is on a per gram basis, which would amount to $ 227 lb^{-1} for the 3-9, and $ 340 lb^{-1} for the 4-9. The prices shown in this row are based on the purchase of $\geq$ 2 lb lots.

(c) Contaminated with a fair amount of zirconium.

Table I-1

COMPARATIVE ANALYTICAL STUDY AND EVALUATION
OF VARIOUS YTTRIA SOURCES

line is still clearly detectable. Consequently, ND for Yb_2O_3 is most likely < 5 ppm.

The penultimate row of Table I-1 indicates the purity with respect to rare earths derived from the results of the analysis carried out in our laboratory. This is an upper value since we have taken the ND rating to be negligible for the calculation. (This assumption may be admissible for 3-9, but is questionable for the higher purity rating.) Nevertheless, it is seen that the derived value of RE-purity tends to fall somewhat short of the purity rating of the manufacturer (see the column headings). This may not be surprising, since such assignments of purity are often estimated only from the kinetic parameters in the ion-exchange purification.

The last row of Table I-1 indicates the price per pound of the powder, which is one of the decisive factors in the choice. The price is a weighting factor since the material chosen must invariably be subjected to in-house purification. The cost of the latter depends not only on the total concentration of impurities, but also on the mass spectrum and the concentration within the collection.

The analyses for alkaline earths in most samples have been carried out and are part of the entry in Table I-1. These impurities are undesirable for crystal growth. Where they have been determined, it is seen that the background is sufficiently large in all cases for the purpose of crystal growth. The alkaline earths can, however, be sufficiently removed by the methods developed in our laboratory. (Such methods were discussed in earlier reports.)

Table I-1 serves as a guide in the first round elimination of samples in the choice of a beginning raw material (for the purpose of crystal growth). Let us adopt as our crux in the final selection the lowest content of Tb_4O_7. It is unfortunate that emission spectrograph becomes inadequate for this purpose,

due to its poor sensitivity. A less sophisticated but more sensitive detection scheme is a visual comparison of the powders. In the oxidized condition, 50 ppm Tb_4O_7 is easily appreciated (yellow to brown tint)[1]. A further stretch in sensitivity to $\lesssim$ 5 ppm Tb_4O_7 is gained by growing a crystal from the undoped powder under oxidizing conditions[2].

By mere comparison of powder tint (comparable oxidation), the following order in decreasing content of Tb_4O_7 is established:

$$\text{Varlacoid (3-9)} > \begin{Bmatrix}\text{MC} & (3\text{-}9)\\ \text{McKay} & (3\text{-}9)\end{Bmatrix} > \text{ROC (3-9)} > \begin{Bmatrix}\text{MC} & (4\text{-}9)\\ \text{Vitro} & (4\text{-}9)\end{Bmatrix} >$$

$$\text{Zuckerman (5-9)} > \begin{Bmatrix}\text{Vitro} & (3\text{-}9)\\ \text{McKay} & (4\text{-}9)\end{Bmatrix} > \begin{Bmatrix}\text{ROC} & (4\text{-}9)\\ \text{Varlacoid} & (5\text{-}9)\end{Bmatrix} > \text{MC (5-9)} .$$

(MC is an abbreviation for Michigan Chemicals and ROC for Research Organic Chemicals.) From the analysis of Table I-1, the color of powder, and the constraint of price (allowing for cost of in-house purification), the choice was narrowed down to two, ROC and Zuckerman. The final selection, based on the color of the boule grown from the undoped powder, showed that ROC(4-9) was more suitable for our purpose.

It is worthwhile to stress that emission spectroscopy alone could not have carried the selection to the degree of refinement

---

[1] The powder should be oxidized. In the reduced form, higher concentration of Tb_4O_7 easily escapes detection. Valance state of the additive plays an extremely important part in such physical methods. A striking example was encountered recently in the case of raw material Gd_2O_3 (4-9). This was highly contaminated with europium present as Eu^{+3}. Consequently, the powder showed no odd tint and the blue fluorescence did not stand out beyond the scattered blue from the UV source. Upon oxidation, the resulting orange fluorescence of Eu^{+3} was manifested in a very striking manner.

[2] Growing a small crystal bead from the undoped powder, followed by redox, UV, and thermal treatments, offers a sensitive detection scheme which has yet to be developed.

called for. This was achieved through an interplay of various in-house capabilities. Considering the uncertainties in the purity assignments from processing (the possible variations in a given product from a given source), it is easily appreciated that such survey studies are extremely limited in time. However, there is no question that such a survey is indeed worthwhile and profitable.

In the way of terminating this presentation on a recent survey study, it would be a gross misinterpretation to take our findings to be a criticism of the various yttria sources. In fact, our results show that there is no great disparity, in general, between the manufacturers' purity rating and that which was obtained by analysis. There is no doubt that such powders are useful for other applications within the accommodation of their purity ratings. However, as we learn more about the crystal growth of Y_2O_3, we begin to appreciate that some impurities are innocuous and others are extremely undesirable. Thus, the spectrum of impurities within the purity rating becomes very significant The constraint of technology and price renders the search for an absolutely clean Y_2O_3 to be a very unrealistic pursuit. Consequently, the highly selective approach is taken, and the value of the survey lies in matching the economics of the outside sources to that of inside (viz., in-house purification) in order to provide the optimum material for crystal growth.

APPENDIX II

Anion and Cation Exchange for the Purification of Yttria

ANION- and CATION-EXCHANGE FOR THE PURIFICATION OF YTTRIA

by

H. Kimura, L. Podoksik, and A. Altmann

For the separation of low atomic number rare earth elements from Y_2O_3, anion exchange resin Dow 1X4, 200-400 mesh was used. The starting powder used in this experiment contained 11 % Dy_2O_3, 0.8 % Tb_4O_7, and 0.45 % Ho_2O_3 (weight basis). Y_2O_3 powder was dissolved in concentrated HNO_3 and mixed with MeOH in 5 vol HNO_3 to 95 vol MeOH.

The weight of Y_2O_3 and the concentrations of each rare earth oxide in Y_2O_3 as a function of the various fractions (eluate) collected are tabulated in Table II-1. A total volume of 1000 cm^3 corresponds to a fraction. High-purity yttria comes through first, and it is seen from the table that the tail end of the elution carries the above-named impurities. (Note the monotonic increase in all three impurities with the later fractions, notwithstanding very slight irregularities in the case of Tb_4O_7.)

The rare earth oxide concentrations in the combined n fractions are also of interest. Table II-2 (derived from Table II-1) lists the calculated concentrations of each rare earth oxide in the yttria derived from the liquor which is made up of the 1st through the nth eluant fraction. The values in Table II-1 for a given fraction are weighted according to the yttria content of the eluant. Note that, if all fractions were combined, no purification is accomplished for Dy or Ho. This is not the case, however, for Tb (one order of magnitude lower than the starting). This suggests that Tb is held most tenaciously by the resin, as compared with Dy or Ho.

For the separation of the higher atomic number rare earth elements, Dow X50 cation exchange resin was used. The starting powder was prepared by doping the high purity Y_2O_3 powder with

Fractions	Wt Y_2O_3 (g) per 1000 cm^3	Wt % Dy_2O_3	Wt % Ho_2O_3	Wt % Tb_4O_7
1, 2 *	0.467	2.0	0.28	0.060
3	5.58	2.0	0.20	0.068
4	6.93	5.0	0.27	0.018
5	8.07	8.2	0.33	0.025
6	6.84	12.	0.67	0.042
7	4.90	12.	0.61	0.15
8	3.07	12.	0.72	0.090
9	2.11	13.	0.76	0.12
10	1.09	14.	0.84	0.19
11	1.02	14.	0.94	0.20
12	0.93	19.	0.92	0.30
13	0.67	18.	0.96	0.38
14	0.21	21.	1.1	0.58

* Fractions 1 and 2 were combined due to the small amount of Y_2O_3 in the first fraction.

Table II-1

IMPURITY CONTENT OF YTTRIA vs FRACTION ELUTED (ANION EXCHANGE)

Number of Fractions Combined	% Recovery of Y_2O_3	Wt % Dy_2O_3	Wt % Ho_2O_3	Wt % Tb_4O_7
1 ~ 2	0.78	2.0	0.28	0.060
1 ~ 3	10.	2.0	0.20	0.068
1 ~ 4	21.	3.6	0.24	0.042
1 ~ 5	35.	5.4	0.28	0.035
1 ~ 6	47.	7.0	0.37	0.037
1 ~ 7	55.	7.8	0.41	0.054
1 ~ 8	60.	8.1	0.44	0.057
1 ~ 9	63.	9.7	0.45	0.061
1 ~ 10	65.	9.5	0.46	0.064
1 ~ 11	67.	9.9	0.48	0.068
1 ~ 12	68.	10.	0.49	0.073
1 ~ 13	70.	10.	0.49	0.078
1 ~ 14	70.	10.	0.50	0.080

Table II-2

INTEGRATED CONTENT IN RARE EARTH OXIDES WITH THE TOTAL ELUANT (ANION EXCHANGE)

1 Wt % each of the following rare earth oxides: Gd_2O_3, Tb_4O_7, Dy_2O_3, Er_2O_3, and Yb_2O_3. 250 cm^3 fractions were collected, evaporated, and the rare earth concentrations in each fraction were determined similarly (emission spectrograph).

The weight of Y_2O_3 and the concentrations of rare earth oxides in each fraction are tabulated in Table II-3. The concentrations of Gd_2O_3, Tb_4O_7, and Dy_2O_3 in each fraction were about 1 % and therefore were not tabulated (i.e., no cleanup effected). In contrast to Table II-1 (anion exchange), it is evident from Table II-3 (cation exchange) that the first fractions must be removed in order to accomplish purification. It should be realized that fraction 1 only refers to the collection where a sensible content of yttria shows up. Hence, in the earlier collections, Yb_2O_3 is eluted out even before any appreciable amount of Y_2O_3 becomes involved.

The calculated rare earth concentrations in the combined fractions, starting from the 8th fraction, are tabulated in Table II-4. Again, the impurity content of each fraction is weighted by the amount of yttria derived from the given fraction.

Fractions	Wt Y_2O_3 (g) per 250 cm^3	Wt % Er_2O_3	Wt % Yb_2O_3
1	0.35	4.4	0.078
2	0.60	2.1	0.022
3	0.68	0.23	0.080
4	0.80	0.26	0.056
5	0.80	0.056	0.015
6	0.70	0.028	0.0090
7	0.60	<0.01	<0.005
8	0.32	<0.01	<0.005

Table II-3

IMPURITY CONTENT OF YTTRIA vs FRACTION ELUTED (CATION EXCHANGE)

Number of Fractions Combined	% Recovery of Y_2O_3	Wt % Er_2O_3	Wt % Yb_2O_3
8	6.4	>0.01	>0.005
8 ~ 7	18.	>0.01	>0.005
8 ~ 6	32.	0.018	0.006
8 ~ 5	48.	0.029	0.009
8 ~ 4	64.	0.087	0.021
8 ~ 3	78.	0.11	0.031
8 ~ 2	90.	0.38	0.031
8 ~ 1	97.	0.67	0.033

Table II-4

INTEGRATED CONTENT IN RARE EARTH OXIDES WITH THE TOTAL ELUANT (CATION EXCHANGE)

APPENDIX III

Empirical Characterization of Flowability

EMPIRICAL CHARACTERIZATION OF FLOWABILITY

by

M. A. Pearson

A study of the kinetics of packing in conjunction with powder technology leads to an appreciation of parameters relevant to a steady-state operation. Characterization of the powder for the purpose of the Verneuil method rests on two impedance parameters: z_p, particle-particle impedance (i.e., friction between particles), and z_s, particle-screen impedance[1].

Previous observations suggest that the desired relationships are:

(a) $z_p \ll z_s$, and

(b) z_s, commensurate with level of flow desired.

The first condition means that the powder should attain steady-state packing within a time interval which is short compared with that corresponding to the transient stage of crystal growth ($\sim$ 1 hr). Thus, the objective is to attain a low value of z_p so that the transient stage of packing is very brief and the flow becomes determined only by z_s (and other impedances in series). To simplify the preliminary study on z_p, we have chosen the case where z_s is infinite (i.e., no flow).

The apparatus is shown in Figure III-1. The powder is loaded inside a graduated cylinder in a fluffy condition and subjected to pulsed sound provided by the loudspeaker head

[1] We neglect at first powder cascade, a phenomenon which occurs outside the hopper assembly. It is due to an accumulation of powder along the gas channel (sticking, rough wall, faulty construction or design, etc.).

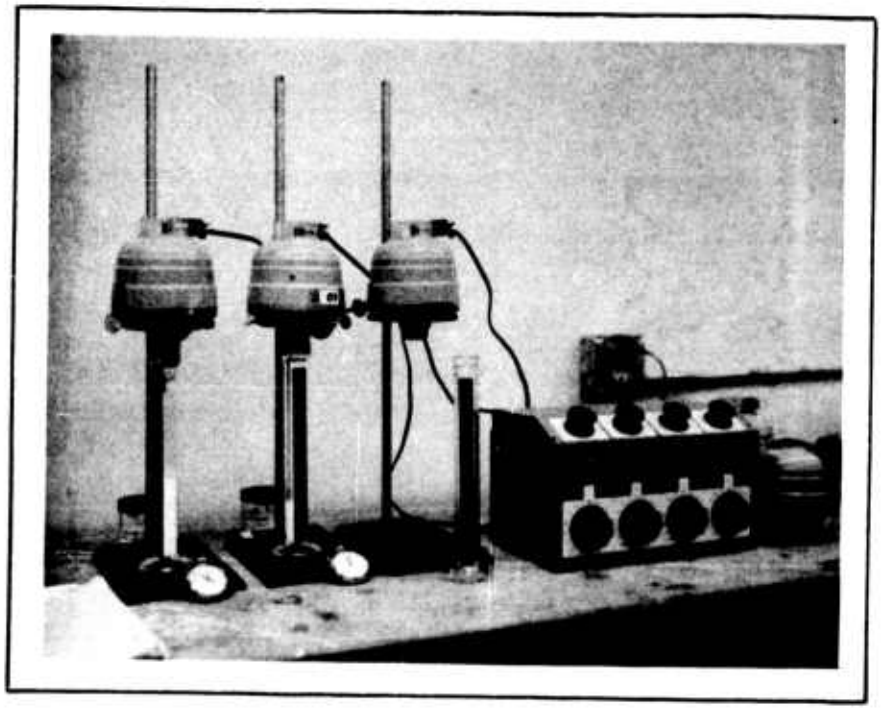

Figure III-1
APPARATUS FOR KINETICS OF POWDER PACKING

which is set on top. (Three such stations are shown.) The repetition rate is chosen so that the period involved is much shorter than the time constant for natural sedimentation. Hence, compacting proceeds at a rate much faster than natural packing.

Observing these limitations in time, the system behaves as if it were subjected to a steady buildup in pressure. A measure of the latter is time, t, since this is proportional to the accumulated effect of the pulsed sound. Since the packing response to each pulse is fast, we can take the (t, v) analog of the (p, v) and characterize the behavior with an "equation of state".

If z_p is large, then "condensation" or limiting packing does not easily occur and the packing behavior should be describable with one equation of state. However, if z_p is small, the "condensed state" comes about early and the behavior breaks away from the description of "one state". The latter is desired, for it is more conducive to steady-state flow, subject only to z_s.[2] These features are shown in Figure III-2, where the time scale is accompanied by another yardstick -- the Verneuil boule.

The two curves shown in Figure III-3 were obtained in a kinetics-of-packing experiment for a powder characterized as "bad flowing" (uncoated Y_2O_3 powder) or "good flowing" (coated Y_2O_3 powder). Coating the powder has greatly reduzed z_p so that "condensation" shows up easily.

By choosing a powder which has a very satisfactory flow property as a reference, packing behavior of other samples can be compared. With t as the parameter, v of the reference is plotted as the abscissa and v of the sample under consideration

[2] If z_p is large, one can still in principle effect $z_s >> z_p$. However, the value of z_s (screen impedance) may be ridiculously high to permit a flow realistic for crystal growth.

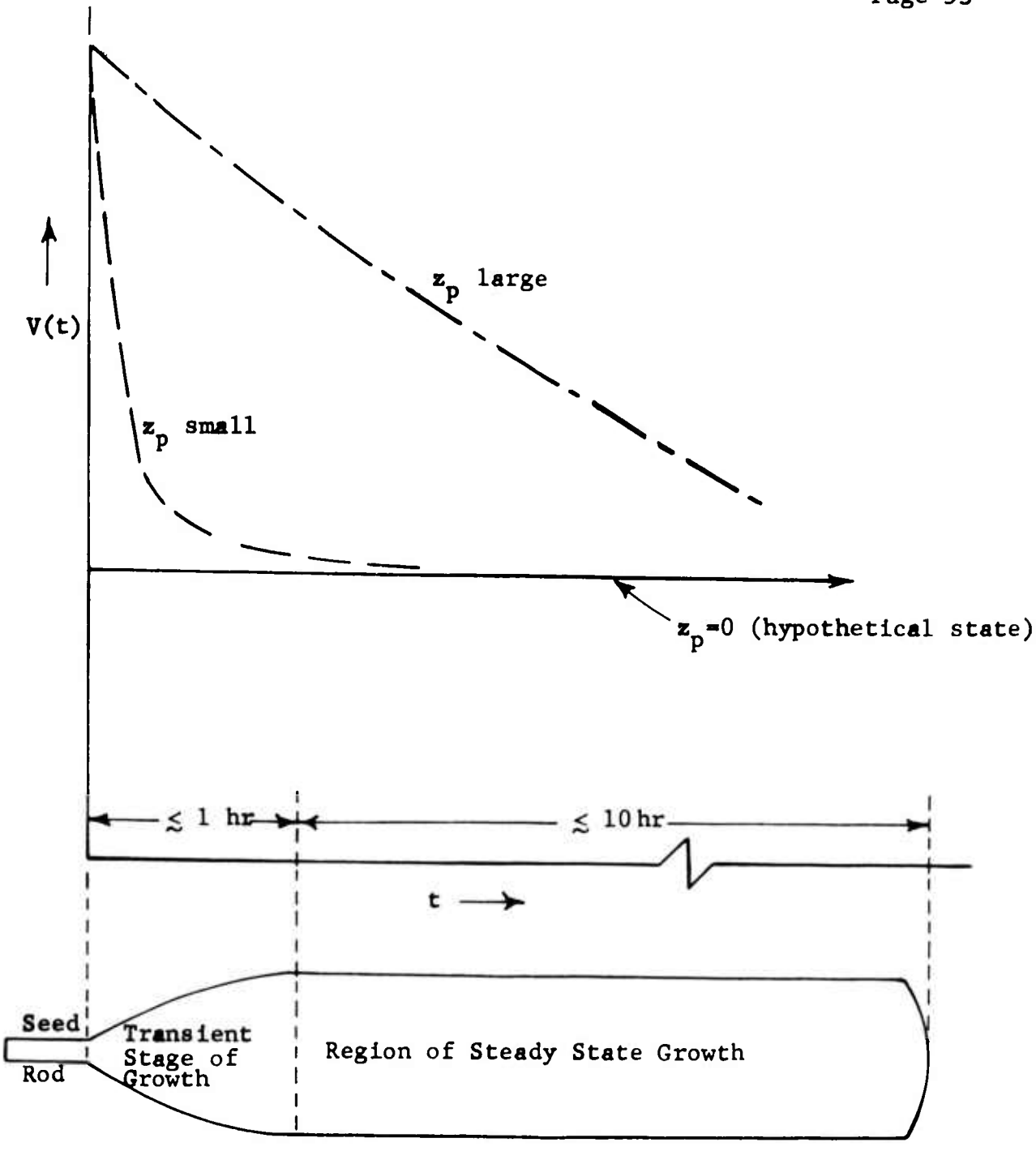

Figure III-2

TIME SCALE FOR POWDER PACKING
SHOWING RELATION TO VERNEUIL CRYSTAL GROWTH
CASE OF z_s INFINITE

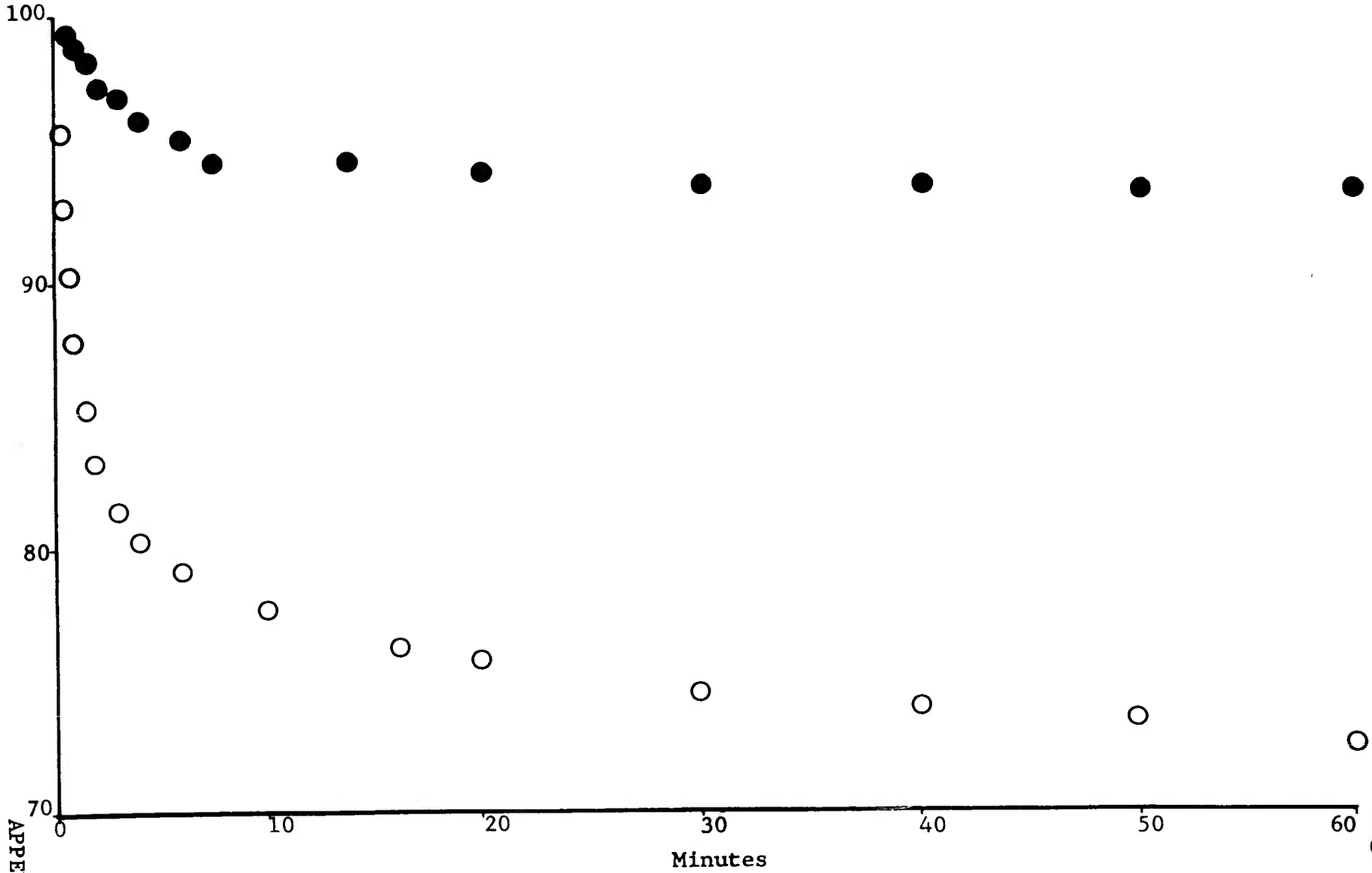

Figure III-3

DYNAMIC PACKING BEHAVIOR OF YTTRIA POWDER
COATED ○ VERSUS THE RAW MATERIAL ●

as the ordinate. Thus, the line passing through the origin with slope = -1 is the reference. Curves above this reference have a z_p greater than the reference (packs slower than the reference). Those below have a z_p lower than the reference (compacts faster than the reference). By this means we can appreciate the dependence of z_p on changes in the surface state of the particle. Again, it is appreciated, from Figure III-4, that the coated yttria powder has the lowest z_p. The reference curves for two raw materials are shown. The flowability of these two raw powders is not quite satisfactory for crystal growth (Verneuil). Raw yttria powder 1 is completely unsuitable for this purpose.

The striking effect of the coat on flowability is seen in Figure III-5. A dramatic increase in z_p follows if the coating is stripped off (uncoated yttria). A slight increase in z_p of the coated powder follows with aging. This may be attributed to a certain degree of moisturizing of the surface (coat).

The packing behavior of YAG ($Y_3Al_5O_{12}$) powder is quite similar to that shown by raw Y_2O_3 (curve 1 in Figure III-4). The powder packs with a small bulk density change. These features are known to be associated with poor flow control (cascading).

It is to be expected that other impedance parameters come into play in the characterization of powder flow for the more realistic cases. The work described above deals with the case where the mass of powder remains constant with time in a sedimentation chamber (i.e., $z_s = \infty$). As a consequence, the kinetics of forced sedimentation yields one impedance parameter, z_p.

The more realistic situations apply to a finite value of z_s, commensurate with the range of level of flow desired. The condition $z_p \ll z_s$ means that the current (powder flow) through

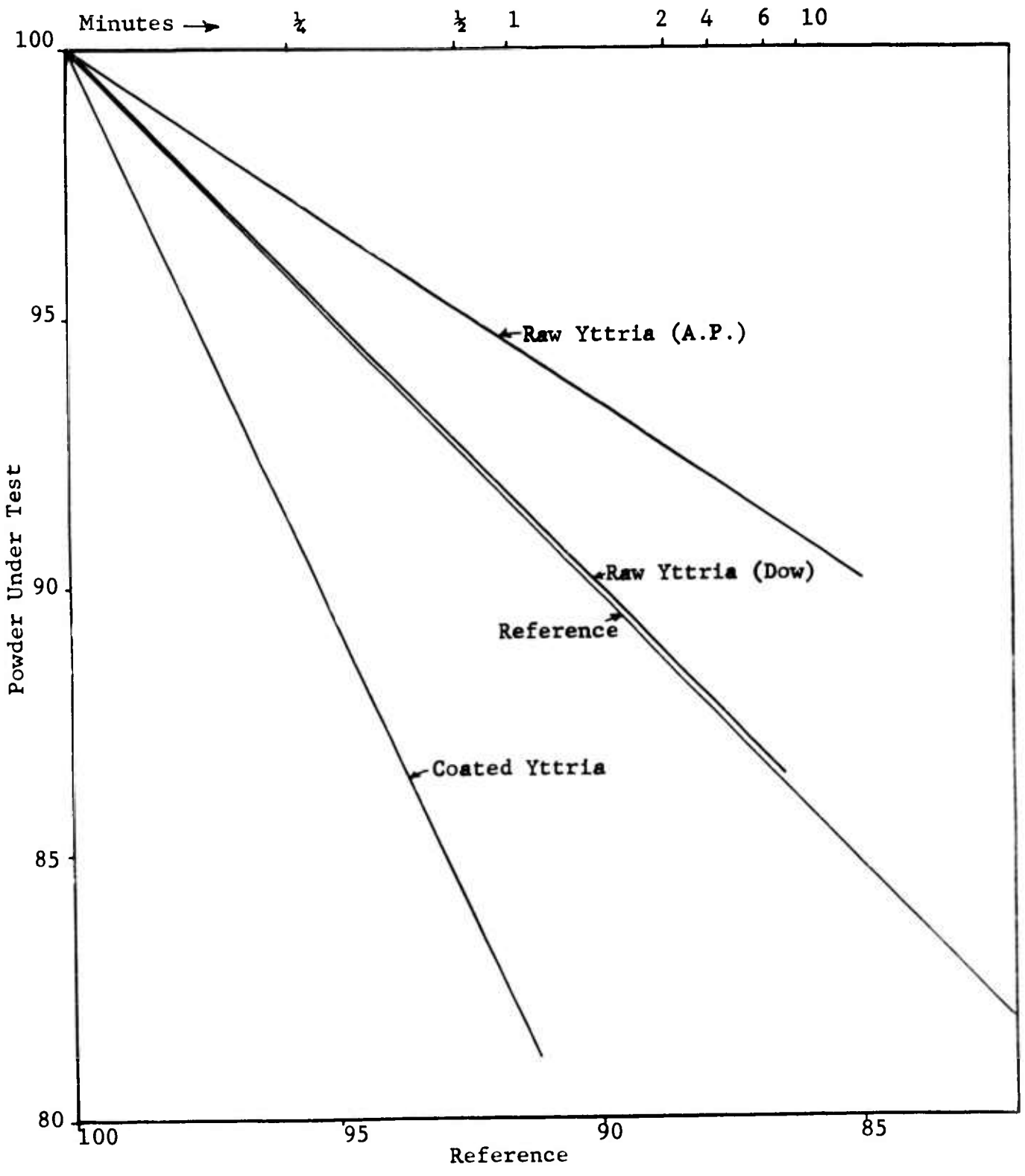

Figure III - 4

COMPARISON OF RELATIVE FLOWABILITY
OF COATED YTTRIA WITH RAW MATERIALS

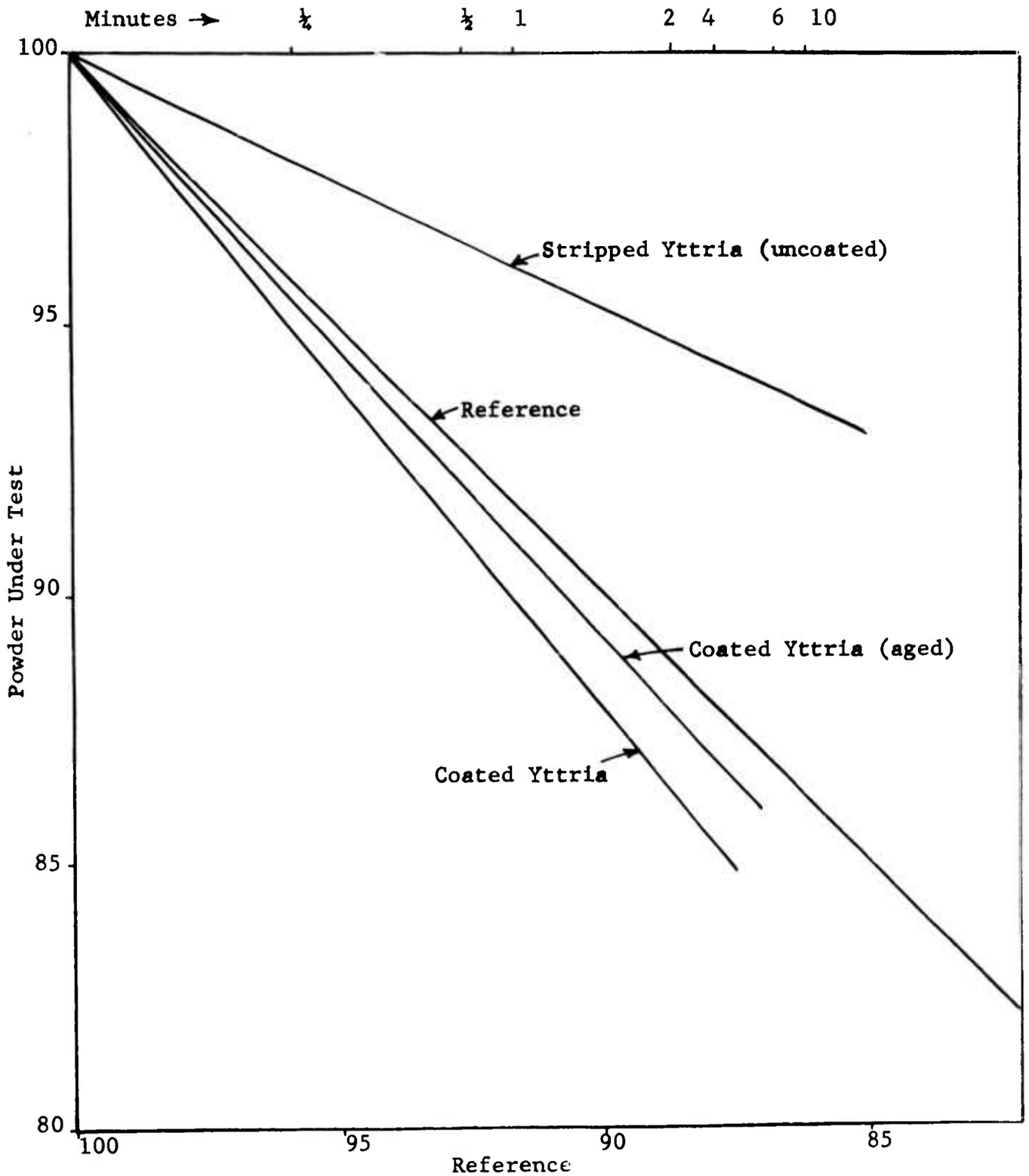

Figure III-5

COMPARISON OF RELATIVE FLOWABILITY
OF YTTRIA - COATED vs STRIPPED (UNCOATED)

the screen could be arranged to be linearly dependent to the driving force (pulsed sound). This feature is important for the purpose of monitoring and controlling powder flow.

In practice, however, the stability of the current (powder flow) leaving the burner nozzle is what really matters. Powder cascade (erratic pulse component in the current) is a phenomenon which occurs outside the hopper. If $z_{s'}$ is an impedance parameter which stands for the friction between the powder and the surface of some material which intervenes (outside of the screen and up to the nozzle), it is seen that $z_p << z_{s'}$ is still the preferred constraint. This discourages powder accummlation along the channel by powder-to-powder sticking. This is no guarantee, however, against cascade -- for there may be ledges or regions faulty in design where accummulation becomes possible due to a sudden change in curvature.

The coefficient of friction or impedance to relative flow between two materials is a function of the nature of the materials and condition of the surface. The latter is affected by thermal treatment, aging, humidification, etc. Obviously, to avoid accummulation and provide proper monitoring of the current, the materials should be chosen such that $z_{s'} < z_s$. At any rate, it should be appreciated that the lowest impedance is z_p (i.e., $z_p << z_{s'} < z_s$). This is tantamount to bestowing on the powder a fair amount of fluidity in the flow behavior. Hence, the emphasis on z_p in the current treatment.

DISTRIBUTION LIST

R S Congleton 1
Aerospace Group
Research & Development Division
Hughes Aircraft Corporation
Culver City California

Basil Curnutte Jr 1
Kansas State University
Manhattan Kansas

G H Dieke 1
Johns Hopkins University
Baltimore 18 Maryland

C H Keller 1
Pek Labs Inc
925 Evelyn Avenue
Sunnyvale California

S P Keller 1
T J Watson Research Center
International Business Machines
Yorktown Heights New York

A Lempicki 1
General Telephone & Electronics Labs
Bayside 60 New York

T C McAvoy 1
Corning Glass Works
Corning New York

W McKusick 1
Apparatus and Optical Division
Eastman Kodak Company
400 Plymouth Avenue N
Rochester 4 New York

O H Nestor 1
Linde Company
1500 Polco Street
Indianapolis 24 Indiana

J W Nielson 1
Airtron Division
Litton Industries
200 East Hanover Avenue
Morris Plains New Jersey

Gerald Oster
Chemistry Department
Polytechnic Institute of Brooklyn
333 Jay Street
Brooklyn 1 New York — 1

David Stockman
Electronics Laboratory
General Electric Company
Syracuse New York — 1

J W Turner
Electronics Division
Westinghouse Electric Corporation
Post Office Box 1896
Baltimore 3 Maryland — 1

R W Young
American Optical Company
Southbridge Massachusetts — 1

Dr Jerald R Izatt
New Mexico State University
University Park New Mexico — 1

Prof A K Kamal
School of Electrical Engineering
Purdue University
Lafayette Indiana — 1

Thomas C Marshall
Department of Electrical Engineering
Columbia University
New York 27 New York — 1

Charles G Naiman
Mithras Inc
Cambridge 39 Massachusetts

Dr J H Schulman
Solid State Division
U S Naval Research Laboratory
Washington 25 DC — 1

Dr Jack A Soules
Physics Department
New Mexico State University
University Park New Mexico — 1

Dr Arden Sher
Varian Associates
611 Hansen Way
Palo Alto California — 1

Dr Robert A Watson
Physical Sciences Division
Office, Chief Research & Development
Army Research Office
Washington 25 DC — 1

Chief Scientist
Attn: Dr Hans K Ziegler
U S Army Electronics Command
Fort Monmouth New Jersey — 1

Director, Institute of Exploratory Research
Attn: Dr E M Reilley
Army Signal Research and Development Laboratory
Fort Monmouth New Jersey — 1

Assistant Director of Surveillance
Attn: Dr Harrison J Merrill
Army Signal Research and Development Laboratory
Fort Monmouth New Jersey — 1

Director of Research and Development
Attn: Mr William D McKnight
Army Ordnance Missile Command
Huntsville Alabama — 1

Office, Chief of Naval Operations
Attn: Mr Ben Rosenberg OP-07I-1
Department of the Navy
Washington 25 DC — 1

Bureau of Naval Weapons
Attn: Dr C H Harry RR-2
Department of the Navy
Washington 25 DC — 1

Bureau of Ships
Attn: Dr G C Sponsler Code 305
Department of the Navy
Washington 25 DC — 1

Department of Naval Research
Attn: Dr Signey Reed Code 402C
Department of the Navy
Washington 25 DC — 1

Office of Naval Research
Attn: Mr Frank B Isakson Code 421
Department of the Navy
Washington 25 DC — 3

Office of Naval Research
Attn: Mr J W Smith Code 406I
Department of the Navy
Washington 25 DC — 1

Naval Research Laboratory
Attn: Dr C C Klick Code 6440
Department of the Navy
Washington 25 DC — 1

Naval Research Laboratory
Attn: Dr L F Drummeter Code 7360
Department of the Navy
Washington 25 DC — 1

Headquarters, USAF
Attn: LtCol E N Myers Code AFRDR-NU-3
Department of the Air Force
Washington DC — 1

Research and Technology Division
Attn: Mr Robert Feik
Bolling AFB
Washington DC — 1

Office of Aerospace Research
Attn: LtCol Ivan Atkinson Code MROSP
Washington 25 DC — 1

Technical Area Manager
Advanced Weapons Division
Aeronautical Systems Division
Attn: Mr Don Newman Code 760A
Wright-Patterson AFB Ohio — 1

Project Engineer
Aerospace Radiation Weapons
Attn: Don Lewis Code 5237
Wright-Patterson AFB Ohio — 1

Air Force Special Weapons Center
Attn: Capt Marvin Atkins Code SWRPA
Kirtland AFB New Mexico — 1

Project Engineer
Attn: Mr Phillip Sandler Code 5561 Comet
Rome Air Development Center
Griffiss AFB New York — 1

Department of Electrical Engineering
Attn: Mr Thomas Henion
New York University, University Heights
New York City New York — 1

BMDR Attn: LtCol W B Lindsay Room 2 B 263, The Pentagon Washingtonn 25 DC	1
Mr John Emmett Physics Department Stanford University Palo Alto California	1
Secretary, Special Group on Optical Masers ODDRCE Advisory Group on Electron Devices 346 Broadway (8th Floor) New York 13 New York	3
Aeronautical Systems Division Attn: ASRCE-31 Wright-Patterson AFB Ohio	1
Dr W Holloway Sperry Rand Research Center Sudbury Massachusetts	1
Technical Area Manager Surveillance Electronic Systems Division Attn:Maj H I Jones Jr Code 760B L G Hanscom AFB Massachusetts	1
Commanding Officer U S Naval Ordnance Laboratory Corona California	1
Director U S Army Engineering Research & Development Labs Attn: Technical Documents Center Fort Belvoir Virginia	1
Office of the Director of Defense Defense Research & Engineering Information Office Library Branch Pentagon Building Washington 25 DC	2
U S Army Research Office Box CM, Duke Station Durham North Carolina	2
Defense Documentation Center Cameron Station Building Alexandria 14 Virginia	20

Director
U S Naval Research Laboratory
Technical Information Officer, Codes 2000, 2021
Washington 25 DC — 6

Commanding Officer
Office of Naval Research Branch Office
230 North Michigan Avenue
Chicago Illinois 60601 — 1

Commanding Officer
Office of Naval Research Branch Office
207 West 24th Street
New York New York 10011 — 1

Commanding Officer
Office of Naval Research Branch Office
1000 Geary Street
San Francisco California 94109 — 1

Air Force Office of Scientific Research
Washington 25 DC — 1

Director
National Bureau of Standards
Washington 25 DC — 1

Director
Research Department
U S Naval Ordnance Laboratory
White Oak, Silver Spring, Maryland — 1

Commanding Officer
Office of Naval Research Branch Office
1030 East Green Street
Pasadena California 91101 — 1

Commanding Officer
Office of Naval Research Branch Office
495 Summer Street
Boston 10 Massachusetts — 1

U S Naval Radiological Defense Laboratory
Attn: Code 941
San Francisco California 94135 — 1

Commanding Officer
U S Army Materials Research Agency
Attn: Technical Library
Watertown Massachusetts 02172 — 1

Boulder Laboratories 1
Attn: Library
National Bureau of Standards
Boulder Colorado

Air Force Weapons Laboratory 1
Attn: Guenther WLRPF
Kirtland AFB New Mexico

Chief, Bureau of Naval Weapons 1
Attn: J M Lee Code RMGA-81
Department of the Navy
Washington 25 DC

Air Force Cambridge Research Laboratories 1
Attn: CRXL-R, Research Library
L G Hanscom Field Massachusetts

Battelle Memorial Institute 1
Attn: BMI-Defender
505 King Avenue
Columbus 1 Ohio

Headquarters, USAELRDL 1
Attn: SELRA/SAR Nr 4, X, and PF
Fort Monmouth New Jersey 07703

Commander 1
U S Naval Ordnance Test Station
Attn: Mr G A Wilkins Code 4041
China Lake California

J C Almasi 1
Advanced Technology Laboratory
General Electric Company
Schnectady New York

Prof Rubin Braunstein 1
Department of Physics
University of California
Los Angeles 24 California

N I Adams 1
Perkin-Elmer Corporation
Norwalk Connecticut

E P Reidel 1
Quantum Electronics Department
Research Laboratories
Westinghouse Electric Corporation
Pittsburgh Pennsylvania

Prof H G Hanson
University of Minnesota
Duluth Minnesota — 1

P Schaffer
Lexington Laboratories Inc
84 Sherman Street
Cambridge Massachusetts — 1

L E Rautiola
Linde Division
Union Carbide Corporation
East Chicago Indiana — 1

F S Galasso
United Aircraft Research Labs
400 Main Street
East Hartford Connecticut — 1

J W Nielson
Airton Division of Litton Industries
Morris Plains New Jersey — 1

E M Flanigen
Linde Company
Division of Union Carbide
Tonawanda New York — 1

W Prindle
American Optical Companh
14 Mechanic Street
Southbridge Massachusetts — 1

R G Meyerland
Plasma Physics
United Aircraft Corporation
East Hartford 8 Connecticut — 1

Prof N Bloembergen
Division of Engineering and Applied Physics
Harvard University
Cambridge 38 Massachusetts — 1

Prof R J Collins
Department of Electrical Engineering
University of Minnesota
Minneapolia 14 Minnesota — 1

Dr Alan Kolb
U S Naval Research Lab
Washington DC — 1

Prof J M Feldman
Department of Electrical Engineering
Carnegie Institute of Technology
Pittsburgh 13 Pennsylvania — 1

Prof Arthur Schawlow
Stanford University
Stanford California — 1

Research Materials Information Center
Oak Ridge National Laboratory
Post Office Box X
Oak Ridge Tennessee 37831 — 1

J-5 Plans and Policy Directorate
Joint Chiefs of Staff
Requirements and Development Division
Attn: Special Projects Branch
Room 2D982 The Pentagon
Washington DC 20301 — 1

Advanced Research Projects Agency
Research and Development Field Unit
APO 143, Box 41
San Francisco California — 1

Advanced Research Projects Agency
Research & Development Field Unit
Attn: Mr Tom Brundage
APO 146, Box 271
San Francisco California — 1

Air Force Materials Laboratory
Air Force Systems Command
Attn: MAAM (Lt Col John H Estess)
Wright-Patterson AFB Ohio 45433 — 1

Dr C H Church
Research Laboratories
Westinghouse Electric Corporation
Pittsburgh 35 Pennsylvania — 1

Prof Donald S McClure
Institute of the Study of Metals
University of Chicago
Chicago 37 Illinois — 1

Dr Daniel Grafstein
Aerospace Group
General Precision Inc
Little Falls New Jersey — 1

Prof R C Ohlmann
Westinghouse Research Laboratories
Pittsburgh Pennsylvania 1

Dr R C Linares
Solid State Materials Branch
Perkin-Elmer Corporation
Norwalk Connecticut 06852 1

Dr J G Atwood
Electro-Optical Division
Perkin-Elmer Corporation
Norwalk Connecticut 1

Prof S Claesson
Uppsala University
Uppsala Sweden 1

* * *

UNCLASSIFIED

BLANK PAGE